



# A Preconditioned implicit Roe's scheme for barotropic flows: towards simulation of cavitation phenomena

Edoardo Sinibaldi, François Beux, Maria Vittoria Salvetti

## ► To cite this version:

Edoardo Sinibaldi, François Beux, Maria Vittoria Salvetti. A Preconditioned implicit Roe's scheme for barotropic flows: towards simulation of cavitation phenomena. RR-4891, INRIA. 2003. inria-00071691

HAL Id: inria-00071691

<https://inria.hal.science/inria-00071691>

Submitted on 23 May 2006

**HAL** is a multi-disciplinary open access archive for the deposit and dissemination of scientific research documents, whether they are published or not. The documents may come from teaching and research institutions in France or abroad, or from public or private research centers.

L'archive ouverte pluridisciplinaire **HAL**, est destinée au dépôt et à la diffusion de documents scientifiques de niveau recherche, publiés ou non, émanant des établissements d'enseignement et de recherche français ou étrangers, des laboratoires publics ou privés.

INSTITUT NATIONAL DE RECHERCHE EN INFORMATIQUE ET EN AUTOMATIQUE

*A Preconditioned implicit Roe's scheme for  
barotropic flows: towards simulation of cavitation  
phenomena*

Edoardo Sinibaldi,  
François Beux,  
Maria Vittoria Salvetti

N° 4891

July 21th, 2003

THÈME 4







# A Preconditioned implicit Roe's scheme for barotropic flows: towards simulation of cavitation phenomena

Edoardo Sinibaldi\*,  
François Beux†,  
Maria Vittoria Salvetti‡

Thème 4 — Simulation et optimisation  
de systèmes complexes  
Projet Smash

Rapport de recherche n° 4891 — July 21th, 2003 — 47 pages

**Abstract:** The discretisation of the Euler equations for a barotropic state law is considered. An upwind scheme based on the definition of a Roe's type matrix is first obtained for this particular hyperbolic problem. A low Mach number asymptotic study is performed both in the continuous and discrete case showing that the discrete solution admits pressure fluctuations in space much larger than those of the exact one. This is the same kind of behaviour observed for the case of a polytropic state law. A preconditioning is then applied such that the obtained discrete formulation has an asymptotic behaviour in agreement with the continuous case. A linearised implicit scheme is defined using the properties of the Roe matrix instead of the first-order homogeneity of the flux function which is not satisfied here. The implicit formulation is also extended to the preconditioned scheme. All the proposed ingredients are validated in the case of a quasi 1-D nozzle flow of a cavitating liquid.

**Key-words:** Barotropic flows, Roe's scheme, compressible low Mach number flows, preconditioning, implicit time advancing

\* Classe di Scienze, Scuola Normale Superiore di Pisa, Piazza dei Cavalieri, 7 56126 Pisa, Italy

† Classe di Scienze, Scuola Normale Superiore di Pisa, Piazza dei Cavalieri, 7 56126 Pisa, Italy

‡ Dipartimento di Ingegneria Aerospaziale, Università di Pisa, Via Caruso, 56122 Pisa, Italy

# Un schéma de Roe implicite préconditionné pour des écoulements barotropiques: vers la simulation de phénomènes de cavitation

**Résumé :** Ce travail concerne la discrétisation des équations d'Euler associées à une loi d'état barotropique. Dans un premier temps, un schéma décentré basé sur la définition d'une matrice de Roe est mis au point pour ce problème hyperbolique particulier. Une étude asymptotique à faible nombre de Mach est ensuite effectuée soit pour le cas continu que discret. Cette étude montre que la solution discrète admet des fluctuations spatiales en pression plus importantes que celles de la solution exacte du problème continu. Il s'agit d'un comportement analogue à celui observé dans le cas d'une loi d'état polytropique. Un préconditionnement est alors appliqué de façon que la formulation discrète aie un comportement asymptotique en accord avec le cas continu. Un schéma implicite linéarisé est alors défini utilisant les propriétés de la matrice de Roe au lieu de l'homogénéité de premier ordre de la fonction de flux, propriété qui n'est pas vérifiée dans notre cas. La formulation implicite est ensuite généralisée au cas du schéma préconditionné. L'ensemble de la formulation numérique a été validée dans le cas quasi 1-D d'un écoulement liquide cavitant dans une tuyère.

**Mots-clés :** Ecoulements barotropiques, schéma de Roe, écoulements compressibles à faible nombre de Mach, préconditionnement, schéma implicite

## Contents

<b>1</b>	<b>Introduction</b>	<b>4</b>
<b>2</b>	<b>Governing equations</b>	<b>5</b>
<b>3</b>	<b>Semi-discrete formulation</b>	<b>6</b>
3.1	Introduction . . . . .	6
3.2	The Roe matrix for barotropic flows . . . . .	7
3.3	Semi-discrete equations . . . . .	8
<b>4</b>	<b>Low Mach number asymptotic study</b>	<b>10</b>
4.1	Introduction . . . . .	10
4.2	Non-dimensionalisation . . . . .	10
4.3	The continuous case . . . . .	10
4.4	The discrete case . . . . .	11
<b>5</b>	<b>Preconditioning for the low Mach number flow</b>	<b>15</b>
5.1	Introduction . . . . .	15
5.2	Preconditioned semi-discrete equations . . . . .	15
5.3	Low Mach number limit of the preconditioned semi-discrete equations . . . . .	17
<b>6</b>	<b>Implicit linearised scheme</b>	<b>21</b>
6.1	Introduction . . . . .	21
6.2	The non-preconditioned case . . . . .	22
6.3	The preconditioned case . . . . .	25
<b>7</b>	<b>1D numerical experiments</b>	<b>27</b>
7.1	Description of the problem . . . . .	27
7.2	Results and discussion . . . . .	30
<b>8</b>	<b>Conclusions</b>	<b>37</b>
<b>A</b>	<b>Proof of Lemma 1</b>	<b>40</b>
<b>B</b>	<b>Proof of Lemma 2</b>	<b>41</b>
<b>C</b>	<b>Numerical implementation of the mixture barotropic law</b>	<b>44</b>

## 1 Introduction

The present work is a preliminary study towards the definition of an efficient numerical framework for accurate simulation of cavitating flows. An accurate computation of cavitating flows appears rather difficult; indeed, one has to deal with unsteady two-phase phenomena in which both incompressible zones (pure liquid) and regions where the flow may become highly supersonic (vapor-liquid mixture) are present in the flow. Furthermore, strong discontinuities with radical changes of the physical quantities occur around the saturation point.

To deal with this type of flows, two opposite ways can be followed: adaptation to the compressible case of numerical methods suitable for incompressible flows, or inversely, adaptation to the low Mach number limit of compressible solver. Pressure-based methods, typically used for incompressible flows, have been extended to the compressible case, for instance, in [9] and [10]. In recent works [22], [19], [2], [13] pressure-based methods have been used to deal with cavitation problem.

On the other hand, standard numerical methods for compressible flows, which are more efficient for high Mach number than the modified pressure-based schemes, fail to compute very low Mach number flows. Indeed, at the low Mach number limit, the numerical difficulties are of two types: first, due to the stiffness of the equations with a very large disparity between acoustic and convective time-scales, the numerical schemes result inefficient. Secondly, the accuracy of the solution is lost when the Mach number tends to zero. An explanation of this behaviour, based on an asymptotic analysis in power of the Mach number for both continuous and discrete equations, is given in [8]. The derivation of a time-preconditioning has been proposed to overcome the convergence difficulties [16]. Moreover, the use of a preconditioning also solves the accuracy problem [17], [21]. Furthermore, since the preconditioning only modifies the numerical dissipation, the scheme remains consistent with the time-dependent equations, and thus, the resulting method can be also used for unsteady flows (see [8], [21]). An explanation of the success of the preconditioned formulation can be obtained by again using an asymptotic analysis in power of the Mach number [8].

Our approach belongs to the second class, i.e. preconditioned compressible solvers.

As for modelling, we adopted an homogeneous-flow cavitation model capable of accounting for thermal effects and the concentration of the active cavitation nuclei, which appeared well suited for the applications of our interest (see [3] and [14] for a more detailed discussion). The model results in a barotropic state law based on the mixture sound speed.

Thus, in the present study the continuity and momentum equations for compressible inviscid flows are considered together with a generic barotropic state law. They are discretised by a finite-volume formulation; fluxes are computed by an upwind scheme based on the definition of a Roe's type matrix [12] for this particular hyperbolic problem.

Then, following [8], the low Mach number behaviour is investigated by an asymptotic study both in the continuous and discrete case. The same kind of result obtained for the case of a polytropic state law in [8] is found in our case also, i.e. the discrete solution admits pressure fluctuations in space much larger than those of the exact one. Thus, the same type preconditioning procedure as in [8] and [21] is formulated for the barotropic case and it is

verified that the obtained discrete formulation has an asymptotic behaviour in agreement with the continuous case.

Finally, as for time advancing, a linearised implicit scheme is proposed, in which the linearisation is based on the properties of the Roe matrix. The implicit formulation is also extended to the preconditioned scheme.

All the proposed ingredients are validated in the case of a quasi 1-D nozzle flow of a cavitating liquid. Although in a simplified context, this test case contains most of the numerical difficulties which characterize the simulation of cavitating flows of practical interest.

## 2 Governing equations

The 1D Euler equations for a force-free fluid, written in conservative form, are considered here:

$$\frac{\partial W}{\partial t} + \frac{\partial F(W)}{\partial x} = 0 \quad (1)$$

where:

$$W = \begin{pmatrix} \rho \\ \rho u \\ \rho e_t \end{pmatrix} \quad F(W) = \begin{pmatrix} \rho u \\ \rho u^2 + p \\ u(\rho e_t + p) \end{pmatrix}$$

$\rho$  is the density,  $u$  is the  $x$ -component of the velocity,  $e_t$  is the total energy per unit mass and  $p$  is the pressure. More specifically, we consider a barotropic fluid, i.e. a fluid whose pressure is linked to the corresponding density by means of a one-to-one correspondence of the form:

$$p = p(\rho) \quad (2)$$

At this stage,  $p$  is assumed derivable and such that  $dp/d\rho > 0$ . Then, once the total enthalpy per unit mass  $h_t = e_t + p/\rho$  has been introduced, the Jacobian  $A(W) = \partial F/\partial W$  can be expressed as follows:

$$A(W) = \begin{pmatrix} 0 & 1 & 0 \\ a^2 - u^2 & 2u & 0 \\ u(a^2 - h_t) & h_t & u \end{pmatrix} \quad (3)$$

in which  $a(\rho) = \sqrt{\frac{dp}{d\rho}}$ .

It is easy to verify that the eigenvalues of  $A$  are  $u$ ,  $u + a$  and  $u - a$  (the same as for the “classical” case of the 1D Euler equations associated with an ideal polytropic state equation) and therefore Eqs. (1) and (2) represent a hyperbolic system of conservation laws.

**Note 1** By virtue of the barotropic state law, the energy equation is decoupled from the rest of the system. Therefore, it is possible to consider a reduced set of governing equations

involving only the mass and momentum balances. In spite of this, we will consider the full problem until Sec. 3.2 in order to keep some degree of generality.

**Note 2** Contrary to the “classical” case, the flux function  $F$  for the present case is not first-order homogeneous:

$$F(W) \neq A(W)W$$

Since the homogeneity property is often used to define specific numerical schemes, the above remark should be kept in mind while generalizing some classical hyperbolic solvers.

### 3 Semi-discrete formulation

#### 3.1 Introduction

In this section a semi-discrete formulation of Eq. (1) is derived. To the purpose, we consider a finite-volume space discretisation of the form:

$$\delta_i \frac{dW_i}{dt} + \Phi_{i(i+1)} - \Phi_{(i-1)i} = 0 \quad (4)$$

where:

- $\delta_i$  is the measure of the  $i$ -th cell;
- $W_i$  is the mean integral value of  $W$  on the  $i$ -th cell;
- $\Phi_{lr}$  is the numerical flux function representing the convective flux flowing from the  $l$ -th (left) cell towards the  $r$ -th (right) one.

Eq. (4) is a semi-discrete equation which can be explicitly written once the numerical flux function has been specified. In the present work we consider the Roe numerical flux function (see [12]):

$$\Phi_{lr} = \frac{F(W_l) + F(W_r)}{2} - \frac{1}{2} |\tilde{A}(W_l, W_r)| (W_r - W_l) \quad (5)$$

where  $\tilde{A}$  is a suitable matrix, called “Roe’s matrix”, verifying the following conditions for any  $(W_l, W_r)$ :

1.  $\tilde{A}(W_l, W_r)$  is diagonalisable with real eigenvalues,
2.  $\lim_{W_l, W_r \rightarrow W^*} \tilde{A}(W_l, W_r) = A(W^*) = \frac{\partial F}{\partial W}(W^*)$ ,
3.  $\tilde{A}(W_l, W_l) (W_r - W_l) = F(W_r) - F(W_l)$ .

Let  $\lambda_1$ ,  $\lambda_2$  and  $\lambda_3$  be the eigenvalues of  $\tilde{A}$ ; then  $\tilde{A} = T \text{Diag}(\lambda_1, \lambda_2, \lambda_3) T^{-1}$  where  $T$  is the (right eigenvectors) similarity matrix. The matrix  $|\tilde{A}|$  in (5) is defined as:  $|\tilde{A}| = T \text{Diag}(|\lambda_1|, |\lambda_2|, |\lambda_3|) T^{-1}$ .

Clearly, the Roe matrix depends in general on the specific problem under consideration and, in particular, on the specific fluid. A Roe matrix  $\tilde{A}$  has initially been introduced in [12] for the case of the Euler equations associated with an ideal polytropic state equation. Different extensions to more complex cases have been proposed in the literature (see e.g. [5], [20], [1] and [7]). In the following, a Roe's matrix is proposed for the problem under consideration and the corresponding semi-discrete equations are explicitly written.

### 3.2 The Roe matrix for barotropic flows

In this subsection we determine a Roe matrix for the 1D Euler equations associated with a generic barotropic fluid, i.e. Eqs. (1) and (2). To the purpose, we recall the well-known “Roe averages” (see [12]):

$$\left\{ \begin{array}{l} \tilde{\rho}(W_l, W_r) = \sqrt{\rho_l \rho_r} \\ \tilde{u}(W_l, W_r) = \frac{\sqrt{\rho_l} u_l + \sqrt{\rho_r} u_r}{\sqrt{\rho_l} + \sqrt{\rho_r}} \\ \tilde{h}_t(W_l, W_r) = \frac{\sqrt{\rho_l} (h_t)_l + \sqrt{\rho_r} (h_t)_r}{\sqrt{\rho_l} + \sqrt{\rho_r}} \end{array} \right. \quad (6)$$

Furthermore, we introduce the following notation:

$$\Delta^{lr}(\cdot) = (\cdot)_r - (\cdot)_l$$

Let us consider, at a preliminary stage, the 1D Euler equations associated with an ideal polytropic state equation. In this case, the Jacobian matrix depends on the variables  $W$  only through the two physical quantities  $u$  and  $h_t$ . The Roe matrix verifies a similar property, indeed (see [12]):

$$\tilde{A}(W_l, W_r) = A(\tilde{u}(W_l, W_r), \tilde{h}_t(W_l, W_r)) \quad (7)$$

with  $\tilde{u}$  and  $\tilde{h}_t$  given by (6). By virtue of the following lemma, whose proof is reported in Sec. A, it is possible to extend Eq.(7) to the problem under consideration. Indeed:

**Lemma 1** *A suitable Roe matrix for the problem under consideration is:*

$$\tilde{A} = \begin{pmatrix} 0 & 1 & 0 \\ \tilde{a}^2 - \tilde{u}^2 & 2\tilde{u} & 0 \\ \tilde{u}(\tilde{a}^2 - \tilde{h}_t) & \tilde{h}_t & \tilde{u} \end{pmatrix} \quad (8)$$

where  $\tilde{u}$  and  $\tilde{h}_t$  are given by (6) and  $\tilde{a}^2$  is defined as follows:

$$\tilde{a}^2(W_l, W_r) = \begin{cases} \frac{\Delta^{lr} p}{\Delta^{lr} \rho} & \text{if } \rho_l \neq \rho_r \\ a^2(\rho, p(\rho)) & \text{if } \rho_l = \rho_r = \rho \end{cases} \quad (9)$$

From (8) it is clear that:

$$\tilde{A}(W_l, W_r) = A(\tilde{u}(W_l, W_r), \tilde{h}_t(W_l, W_r), \tilde{a}^2(W_l, W_r)) \quad (10)$$

where  $A = A(u, h_t, a^2)$  is given by (3). The formal analogy between Eqs.(7) and (10) is then evident.

**Note 3** It is possible to derive (6), (8) and (9) from the Roe averages defined in [5] in a more general context. More precisely, in [5] the 1-D Euler equations are considered with a generic state equation of the form:  $p = p(\rho, e)$ ,  $e$  being the internal energy per unit mass, assuming the hyperbolicity of the resulting system and the existence and the unicity of the the associated Riemann problem. Furthermore, (9) has been previously obtained in [6], but only on the reduced problem (11).

**Note 4** As far as the numerical implementation is concerned,  $\tilde{a}^2(W_l, W_r)$  should be defined as follows:

$$\tilde{a}^2(W_l, W_r) = \begin{cases} \frac{\Delta^{lr} p}{\Delta^{lr} \rho} & \text{if } |\Delta^{lr} \rho| > \epsilon \\ a^2(\bar{\rho}_{lr}, p(\bar{\rho}_{lr})) & \text{if } |\Delta^{lr} \rho| < \epsilon \end{cases}$$

where  $\epsilon$  is a suitable numerical threshold and  $\bar{\rho}_{lr}$  is an average value such that:

$$\lim_{W_l, W_r \rightarrow W^*} \bar{\rho}_{lr} = \rho^*$$

For instance, we can take  $\bar{\rho}_{lr} = \tilde{\rho}(W_l, W_r)$  as in (6).

### 3.3 Semi-discrete equations

From now on attention is focused on the "reduced" problem:

$$\frac{\partial}{\partial t} \begin{pmatrix} \rho \\ \rho u \end{pmatrix} + \frac{\partial}{\partial x} \begin{pmatrix} \rho u \\ \rho u^2 + p \end{pmatrix} = 0 \quad (11)$$

associated with a generic barotropic state law like Eq.(2).

In this section we explicitly write the semi-discrete equations:

$$\delta_i \frac{dW_i}{dt} + \Phi_{i(i+1)} - \Phi_{(i-1)i} = 0 \quad (12)$$

where:

- $W_i$  and  $\Phi_{ij}$  now belong to  $\mathbb{R}^2$ ;
- $\Phi_{ij}$  is the Roe flux function (see (5)):

$$\Phi_{ij} = \frac{F(W_i) + F(W_j)}{2} - \frac{1}{2} |\tilde{A}_{ij}| \Delta^{ij} W \quad (13)$$

in which  $\tilde{A}_{ij} = \tilde{A}(W_i, W_j)$  is the reduced Roe matrix from (8), i.e.:

$$\tilde{A}_{ij} = \begin{pmatrix} 0 & 1 \\ \tilde{a}_{ij}^2 - \tilde{u}_{ij}^2 & 2\tilde{u}_{ij} \end{pmatrix}$$

where  $\tilde{a}_{ij} = \tilde{a}(W_i, W_j)$  and  $\tilde{u}_{ij} = \tilde{u}(W_i, W_j)$ .

The eigenvalues of  $\tilde{A}_{ij}$  are:

$$\lambda_{ij}^{(1)} = \tilde{u}_{ij} + \tilde{a}_{ij} \quad \lambda_{ij}^{(2)} = \tilde{u}_{ij} - \tilde{a}_{ij}$$

while the corresponding (right) eigenvectors are  $R_{ij}^{(1)} = (1, \lambda_{ij}^{(1)})^T$  and  $R_{ij}^{(2)} = (1, \lambda_{ij}^{(2)})^T$ . The upwind term of the numerical flux function can then be expressed as:

$$|\tilde{A}_{ij}| \Delta^{ij} W = \sum_{k=1}^2 c_k(\Delta^{ij} W) |\lambda_{ij}^{(k)}| R_{ij}^{(k)}$$

where  $c_k(\bar{v})$  is the  $k$ -th coordinate of  $\bar{v} \in \mathbb{R}^2$  in the basis formed by the eigenvectors. By exploiting the following classical property of the Roe averages (see, for instance, [20] or [1]):

$$\Delta^{ij}(\rho u) = \tilde{u}_{ij} \Delta^{ij} \rho + \tilde{\rho}_{ij} \Delta^{ij} u$$

we obtain:

$$\begin{cases} c_1(\Delta^{ij} W) = \frac{1}{2} \left( \Delta^{ij} \rho + \frac{\tilde{\rho}_{ij}}{\tilde{a}_{ij}} \Delta^{ij} u \right) = \frac{1}{2\tilde{a}_{ij}} \left( \frac{\Delta^{ij} p}{\tilde{a}_{ij}} + \tilde{\rho}_{ij} \Delta^{ij} u \right) \\ c_2(\Delta^{ij} W) = \frac{1}{2} \left( \Delta^{ij} \rho - \frac{\tilde{\rho}_{ij}}{\tilde{a}_{ij}} \Delta^{ij} u \right) = \frac{1}{2\tilde{a}_{ij}} \left( \frac{\Delta^{ij} p}{\tilde{a}_{ij}} - \tilde{\rho}_{ij} \Delta^{ij} u \right) \end{cases}$$

Hence:

$$|\tilde{A}_{ij}| \Delta^{ij} W = \frac{1}{2\tilde{a}_{ij}} U_{ij} \begin{pmatrix} \Delta^{ij} p \\ \tilde{\rho}_{ij} \Delta^{ij} u \end{pmatrix}$$

where:

$$U_{ij} = \begin{pmatrix} \frac{|\lambda_{ij}^{(1)}| + |\lambda_{ij}^{(2)}|}{\tilde{a}_{ij}} & |\lambda_{ij}^{(1)}| - |\lambda_{ij}^{(2)}| \\ \frac{\lambda_{ij}^{(1)} |\lambda_{ij}^{(1)}| + \lambda_{ij}^{(2)} |\lambda_{ij}^{(2)}|}{\tilde{a}_{ij}} & \lambda_{ij}^{(1)} |\lambda_{ij}^{(1)}| - \lambda_{ij}^{(2)} |\lambda_{ij}^{(2)}| \end{pmatrix} \quad (14)$$

By substituting the relevant terms into Eq.(12), the semi-discrete equations finally write:

$$\begin{aligned} 2\delta_i \frac{d}{dt} \begin{pmatrix} \rho_i \\ \rho_i u_i \end{pmatrix} &= \begin{pmatrix} \rho_{i-1} u_{i-1} \\ \rho_{i-1} u_{i-1}^2 + p_{i-1} \end{pmatrix} - \begin{pmatrix} \rho_{i+1} u_{i+1} \\ \rho_{i+1} u_{i+1}^2 + p_{i+1} \end{pmatrix} + \\ \frac{1}{2\tilde{a}_{i(i+1)}} U_{i(i+1)} \begin{pmatrix} \Delta^{i(i+1)} p \\ \tilde{\rho}_{i(i+1)} \Delta^{i(i+1)} u \end{pmatrix} - \frac{1}{2\tilde{a}_{(i-1)i}} U_{(i-1)i} \begin{pmatrix} \Delta^{(i-1)i} p \\ \tilde{\rho}_{(i-1)i} \Delta^{(i-1)i} u \end{pmatrix} \end{aligned} \quad (15)$$

## 4 Low Mach number asymptotic study

### 4.1 Introduction

It is well known from the literature that the accuracy of a compressible flow solver dealing with a nearly incompressible flow is generally very poor. In the present section we analyze the behaviour of both the continuous and the semi-discrete governing equations when the Mach number tends to zero. We will show that the numerical solution may exhibit pressure fluctuations in space much higher than those in the continuous solution. In Sec. 5 a preconditioning technique able to counteract this discrepancy will be introduced.

### 4.2 Non-dimensionalisation

In order to emphasize the role of the Mach number (i.e. of the flow compressibility), the governing equations must be non-dimensionalised. To the purpose, we introduce the following reference quantities:

$$\rho_* = \max_x \rho(x, 0), u_* = \max_x u(x, 0), a_*^2 = \max_x a^2(x, 0) \text{ and } \delta_* \text{ (an arbitrary length scale).}$$

Then, a reference Mach number may be defined as:  $M_* = u_*/a_*$  where  $a_* = \sqrt{a_*^2}$ . By exploiting these quantities, we define the non-dimensional variables as:  $x' = x/\delta_*$ ,  $\rho' = \rho/\rho_*$ ,  $u' = u/u_*$ ,  $t' = tu_*/\delta_*$  and  $p' = p/(\rho_* a_*^2)$ . These variables will be used for both the continuous and the semi-discrete flow equations (in the latter case the discretised variables will be non-dimensionalised). The prime will be dropped for the sake of clarity.

### 4.3 The continuous case

By introducing the non-dimensional variables into the mass and momentum balances of Eq.(1), the following system is obtained:

$$\frac{\partial}{\partial t} \begin{pmatrix} \rho \\ \rho u \end{pmatrix} + \frac{\partial}{\partial x} \begin{pmatrix} \rho u \\ \rho u^2 + \frac{1}{M_*^2} p \end{pmatrix} = 0 \quad (16)$$

while the non-dimensional state law is still of the form of Eq.(2). We now look for solutions to Eq.(16) as an asymptotic expansion in power of  $M_*$ :

$$\begin{cases} \rho(x, t) = \rho_0(x, t) + M_* \rho_1(x, t) + M_*^2 \rho_2(x, t) + \dots \\ u(x, t) = u_0(x, t) + M_* u_1(x, t) + M_*^2 u_2(x, t) + \dots \\ p(x, t) = p_0(x, t) + M_* p_1(x, t) + M_*^2 p_2(x, t) + \dots \end{cases} \quad (17)$$

By substituting these expansions into (16), the momentum equation can be rewritten as follows:

$$\frac{1}{M_*^2} \frac{\partial p_0}{\partial x} + \frac{1}{M_*} \frac{\partial p_1}{\partial x} + \left( \frac{\partial \rho_0 u_0}{\partial t} + \frac{\partial p_2}{\partial x} + \rho_0 u_0^2 \right) + M_* (\dots) = 0$$

It is possible to solve this equation in the limit  $M_* \rightarrow 0$  only if:

$$\frac{\partial p_0}{\partial x} = \frac{\partial p_1}{\partial x} = 0 \quad (18)$$

As a consequence, *when  $M_* \rightarrow 0$  the pressure field solution of Eq.(16) is of the form:*

$$p(x, t) = p_0(t) + M_* p_1(t) + M_*^2 \hat{p}_2(x, t) \quad (19)$$

**Note 5** Since the fluid is barotropic, it is possible to write:

$$p = p(\rho) = p(\rho_0 + M_* \rho_1 + M_*^2 \dots) = p(\rho_0) + M_* a^2(\rho_0) \rho_1 + M_*^2 \dots$$

By comparing this Taylor expansion with (17) we get:

$$\begin{cases} p_0 = p(\rho_0) \\ p_1 = a^2(\rho_0) \rho_1 \end{cases} \quad (20)$$

#### 4.4 The discrete case

In the low Mach number limit ( $M_* \rightarrow 0$ )  $|\tilde{a}_{ij}| > |\tilde{u}_{ij}|$ . Therefore, since  $\tilde{a}_{ij} > 0$ , we have  $|\lambda_{ij}^{(1)}| = \lambda_{ij}^{(1)}$ ,  $|\lambda_{ij}^{(2)}| = -\lambda_{ij}^{(2)}$  and thus, (14) becomes:

$$U_{ij} = 2 \begin{pmatrix} 1 & \tilde{u}_{ij} \\ 2\tilde{u}_{ij} & (\tilde{u}_{ij}^2 + \tilde{a}_{ij}^2) \end{pmatrix} \quad (21)$$

By substituting (21) into Eq.(15) we get the following semi-discrete equations:

$$\begin{aligned} 2\delta_i \frac{d\rho_i}{dt} &= (\rho_{i-1} u_{i-1} - \rho_{i+1} u_{i+1}) + \left( \frac{\Delta^{i(i+1)} p}{\tilde{a}_{i(i+1)}} - \frac{\Delta^{(i-1)i} p}{\tilde{a}_{(i-1)i}} \right) + \\ &\quad \left( \frac{u^{i(i+1)}}{\tilde{a}_{i(i+1)}} \tilde{\rho}_{i(i+1)} \Delta^{i(i+1)} u - \frac{u^{(i-1)i}}{\tilde{a}_{(i-1)i}} \tilde{\rho}_{(i-1)i} \Delta^{(i-1)i} u \right) \end{aligned} \quad (22)$$

$$\begin{aligned}
2\delta_i \frac{d\rho_i u_i}{dt} = & (\rho_{i-1} u_{i-1}^2 - \rho_{i+1} u_{i+1}^2) \\
& + (p_{i-1} - p_{i+1}) + 2 \left( \frac{\tilde{u}_{i(i+1)}}{\tilde{a}_{i(i+1)}} \Delta^{i(i+1)} p - \frac{\tilde{u}_{(i-1)i}}{\tilde{a}_{(i-1)i}} \Delta^{(i-1)i} p \right) + \\
& (\tilde{a}_{i(i+1)} \tilde{\rho}_{i(i+1)} \Delta^{i(i+1)} u - \tilde{a}_{(i-1)i} \tilde{\rho}_{(i-1)i} \Delta^{(i-1)i} u) \\
& + \left( \frac{\tilde{u}_{i(i+1)}}{\tilde{a}_{i(i+1)}} \tilde{u}_{i(i+1)} \tilde{\rho}_{i(i+1)} \Delta^{i(i+1)} u - \frac{\tilde{u}_{(i-1)i}}{\tilde{a}_{(i-1)i}} \tilde{u}_{(i-1)i} \tilde{\rho}_{(i-1)i} \Delta^{(i-1)i} u \right)
\end{aligned} \tag{23}$$

Eqs. (22) and (23) are then non-dimensionalised by means of the reference variables introduced in Sec. 4.2. Consequently, the non-dimensionalised Roe averages are obtained as follows:  $\tilde{\rho}_{ij} = \rho_\star \tilde{\rho}'_{ij}$ ,  $\tilde{u}_{ij} = u_\star \tilde{u}'_{ij}$  and  $\tilde{a}_{ij} = a_\star \tilde{a}'_{ij}$ . As a result, the following non-dimensional semi-discrete equations are obtained (the prime is dropped for the sake of clarity):

$$\begin{aligned}
2\delta_i \frac{d\rho_i}{dt} = & (\rho_{i-1} u_{i-1} - \rho_{i+1} u_{i+1}) + \frac{1}{M_\star} \left( \frac{\Delta^{i(i+1)} p}{\tilde{a}_{i(i+1)}} - \frac{\Delta^{(i-1)i} p}{\tilde{a}_{(i-1)i}} \right) \\
& + M_\star \left( \frac{u^{i(i+1)}}{\tilde{a}_{i(i+1)}} \tilde{\rho}_{i(i+1)} \Delta^{i(i+1)} u - \frac{u^{(i-1)i}}{\tilde{a}_{(i-1)i}} \tilde{\rho}_{(i-1)i} \Delta^{(i-1)i} u \right)
\end{aligned} \tag{24}$$

$$\begin{aligned}
2\delta_i \frac{d\rho_i u_i}{dt} = & (\rho_{i-1} u_{i-1}^2 - \rho_{i+1} u_{i+1}^2) \\
& + \frac{1}{M_\star^2} (p_{i-1} - p_{i+1}) + \frac{2}{M_\star} \left( \frac{\tilde{u}_{i(i+1)}}{\tilde{a}_{i(i+1)}} \Delta^{i(i+1)} p - \frac{\tilde{u}_{(i-1)i}}{\tilde{a}_{(i-1)i}} \Delta^{(i-1)i} p \right) + \\
& \frac{1}{M_\star} \left( \tilde{a}_{i(i+1)} \tilde{\rho}_{i(i+1)} \Delta^{i(i+1)} u - \tilde{a}_{(i-1)i} \tilde{\rho}_{(i-1)i} \Delta^{(i-1)i} u \right) \\
& + M_\star \left( \frac{\tilde{u}_{i(i+1)}}{\tilde{a}_{i(i+1)}} \tilde{u}_{i(i+1)} \tilde{\rho}_{i(i+1)} \Delta^{i(i+1)} u - \frac{\tilde{u}_{(i-1)i}}{\tilde{a}_{(i-1)i}} \tilde{u}_{(i-1)i} \tilde{\rho}_{(i-1)i} \Delta^{(i-1)i} u \right)
\end{aligned} \tag{25}$$

As for the continuous case, we look for semi-discrete solutions to Eqs.(24) and (25) as an asymptotic expansion in power of  $M_\star$ :

$$\begin{cases} \rho_i(t) = \rho_{0i}(t) + M_\star \rho_{1i}(t) + M_\star^2 \rho_{2i}(t) + \dots \\ u_i(t) = u_{0i}(t) + M_\star u_{1i}(t) + M_\star^2 u_{2i}(t) + \dots \\ p_i(t) = p_{0i}(t) + M_\star p_{1i}(t) + M_\star^2 p_{2i}(t) + \dots \end{cases} \tag{26}$$

**Note 6** The power expansion (26) is applied to the Roe averages as well. Let us consider, as an example, the expansion of  $\tilde{a}_{ij}$ . As shown in A,  $\tilde{a}_{ij}$  is always strictly positive. Hence,

$$\tilde{a}_{0ij} = \tilde{a}_{ij}|_{M_\star=0} > 0$$

and  $\tilde{a}_{ij}^{-1}$  may be expanded as follows:

$$\frac{1}{\tilde{a}_{ij}} = \frac{1}{\tilde{a}_{0ij}} \left( 1 + M_* \frac{\tilde{a}_{1ij}}{\tilde{a}_{0ij}} + \dots \right)^{-1} = \frac{1}{\tilde{a}_{0ij}} \left( 1 - M_* \frac{\tilde{a}_{1ij}}{\tilde{a}_{0ij}} + \dots \right)$$

More precisely,  $\tilde{a}_{0ij}$  can be explicitly written as follows:

- if  $\Delta^{ij}\rho = 0$  then  $\rho_i = \rho_j = \bar{\rho}$  and  $\tilde{a}_{ij} = a(\bar{\rho})$ :

$$\tilde{a}_{ij} = a(\bar{\rho}_0) + \frac{da}{d\rho}(\bar{\rho}_0)\bar{\rho}_1 M_* + \dots$$

Clearly,  $\tilde{a}_{0ij} = a(\bar{\rho}_0)$ ;

- if  $\Delta^{ij}\rho \neq 0$  then, by definition:  $\Delta^{ij}\rho\tilde{a}_{ij}^2 = \Delta^{ij}p$ ; if we consider only the terms of order zero in the expansion in power of  $M_*$ , we obtain:  $\Delta^{ij}\rho_0\tilde{a}_{ij}^2 = \Delta^{ij}p_0$ . Since, as previously pointed out,  $\tilde{a}_{0ij}^2 > 0$ , the following equivalence holds:

$$\forall i, j \quad \Delta^{ij}\rho_0 = 0 \Leftrightarrow \Delta^{ij}p_0 = 0$$

- if  $\Delta^{ij}\rho_0 \neq 0$ , and, thus,  $\Delta^{ij}p_0 \neq 0$ , then:

$$\begin{aligned} \tilde{a}_{ij} &= \left( \frac{\Delta^{ij}p}{\Delta^{ij}\rho} \right)^{\frac{1}{2}} \\ &= \left( \frac{\Delta^{ij}p_0}{\Delta^{ij}\rho_0} \right)^{\frac{1}{2}} \left( 1 + \frac{\Delta^{ij}p_1}{\Delta^{ij}p_0} M_* + \dots \right)^{\frac{1}{2}} \left( 1 + \frac{\Delta^{ij}\rho_1}{\Delta^{ij}\rho_0} M_* + \dots \right)^{-\frac{1}{2}} \\ &= \left( \frac{\Delta^{ij}p_0}{\Delta^{ij}\rho_0} \right)^{\frac{1}{2}} + \frac{1}{2} \left( \frac{\Delta^{ij}p_0}{\Delta^{ij}\rho_0} \right)^{\frac{1}{2}} \left( \frac{\Delta^{ij}p_1}{\Delta^{ij}p_0} - \frac{\Delta^{ij}\rho_1}{\Delta^{ij}\rho_0} \right) M_* + \dots \end{aligned}$$

In this case  $\tilde{a}_{0ij} = \left( \frac{\Delta^{ij}p_0}{\Delta^{ij}\rho_0} \right)^{\frac{1}{2}}$ ;

- if  $\Delta^{ij}\rho_0 = 0$  and, thus  $\Delta^{ij}p_0 = 0$ , then, by exploiting the same kind of linearisation as above:

$$\tilde{a}_{0ij} = \left( \frac{\Delta^{ij}p_s}{\Delta^{ij}\rho_s} \right)^{\frac{1}{2}}$$

where  $s$  is the first integer such that  $\Delta^{ij}\rho_s \neq 0$ .

As for the continuous case, once the expansions have been introduced into Eqs. (24) and (25), all the terms associated with  $M_*^{-2}$  and  $M_*^{-1}$  must be set to zero in order to find the asymptotic solution. The resulting equations are:

1. order  $M_\star^{-2}$  (momentum):

$$p_{0(i+1)} - p_{0(i-1)} = 0 \quad (27)$$

2. order  $M_\star^{-1}$  (mass):

$$\frac{\Delta^{i(i+1)} p_0}{\tilde{a}_{0i(i+1)}} - \frac{\Delta^{(i-1)i} p_0}{\tilde{a}_{0(i-1)i}} = 0 \quad (28)$$

3. order  $M_\star^{-1}$  (momentum):

$$\begin{aligned} & 2 \left( \tilde{u}_{0i(i+1)} \frac{\Delta^{i(i+1)} p_0}{\tilde{a}_{0i(i+1)}} - \tilde{u}_{0(i-1)i} \frac{\Delta^{(i-1)i} p_0}{\tilde{a}_{0(i-1)i}} \right) \\ & + (\tilde{a}_{0i(i+1)} \tilde{\rho}_{0i(i+1)} \Delta^{i(i+1)} u_0 - \tilde{a}_{0(i-1)i} \tilde{\rho}_{0(i-1)i} \Delta^{(i-1)i} u_0) \\ & + (p_{1(i+1)} - p_{1(i-1)}) = 0 \end{aligned} \quad (29)$$

By combining Eqs.(27) and (28) we obtain:

$$\left( \frac{1}{\tilde{a}_{0(i-1)i}} + \frac{1}{\tilde{a}_{0i(i+1)}} \right) \Delta^{(i-1)i} p_0 = 0$$

Since  $\tilde{a}_{0ij} > 0$  (as remarked in Note 6), it is possible to conclude that  $p_i$  does not depend on the nodal index  $i$ :

$$p_{0i}(t) = p_0(t)$$

As a consequence,  $\rho_{0i}(t) = \rho_0(t)$  and Eq.(29) reduces to:

$$\tilde{\rho}_0 \left( \tilde{a}_{0i(i+1)} \Delta^{i(i+1)} u_0 - \tilde{a}_{0(i-1)i} \Delta^{(i-1)i} u_0 \right) + (p_{1(i+1)} - p_{1(i-1)}) = 0$$

This equation implies that in general  $p_{1i} = p_{1i}(t)$ . Therefore, *when  $M_\star \rightarrow 0$  the pressure solution to Eqs. (24) and (25) is of the form:*

$$p_i(t) = p_0(t) + M_\star \hat{p}_{1i}(t) \quad (30)$$

By comparing (30) and (19), it is clear that the asymptotic solution to the numerical problem may exhibit a behavior which is remarkably different from that of the continuous solution. The same asymptotic behaviors have been found by Guillard (see [8]) for the case of an ideal polytropic state equation.

The present result shows that the accuracy of a compressible solvers can be dramatically reduced when the flow tends to be (even locally) incompressible.

## 5 Preconditioning for the low Mach number flow

### 5.1 Introduction

In the present section we still concentrate on the semi-discrete problem, i.e. Eq.(12). In order to make the discrete solution recover the same behavior as the continuous one in the low Mach number limit, a modified numerical flux function is introduced. More specifically, the same procedure as in [8] is followed and (13) is replaced with:

$$\Phi_{ij} = \frac{F(W_i) + F(W_j)}{2} - \frac{1}{2} P_{ij}^{-1} |P_{ij}\tilde{A}_{ij}| \Delta^{ij} W \quad (31)$$

where  $P_{ij}$  is the preconditioning matrix, which is, as usual practice, first derived in primitive variables. In our case the simplest choice is:

$$P(W_p) = \begin{pmatrix} \beta^2 & 0 \\ 0 & 1 \end{pmatrix}$$

where the primitive variables are  $W_p = (P, u)^T$  and  $\beta^2$  is a positive real constant. By performing the appropriate change of variables,  $P(W)$  can be expressed as follows:

$$P(W) = \frac{\partial W}{\partial W_p} P(W_p) \frac{\partial W_p}{\partial W} = \begin{pmatrix} \beta^2 & 0 \\ u(\beta^2 - 1) & 1 \end{pmatrix}$$

Finally, we obtain the following expression for the preconditioning matrix:

$$P_{ij} = \begin{pmatrix} \beta^2 & 0 \\ \tilde{u}_{ij}(\beta^2 - 1) & 1 \end{pmatrix} \quad (32)$$

Note that, in the formulation (31), only the dissipative part of the numerical flux is modified, and therefore the numerical scheme remains a consistent approximation of the time-dependent compressible Euler equations.

### 5.2 Preconditioned semi-discrete equations

By substituting the (new) relevant terms into Eq.(12), we obtain a new set of semi-discrete equations. To the purpose, we follow the same procedure as in Sec. 3.3.

The eigenvalues of  $P_{ij}\tilde{A}_{ij}$  are:

$$\lambda_{ij}^{(1)p} = \frac{1 + \beta^2}{2} \tilde{u}_{ij} + \sqrt{X_{ij}} \quad \lambda_{ij}^{(2)p} = \frac{1 + \beta^2}{2} \tilde{u}_{ij} - \sqrt{X_{ij}}$$

where:

$$X_{ij} = \left( \left( \frac{1 - \beta^2}{2} \right) \tilde{u}_{ij} \right)^2 + \beta^2 \tilde{a}_{ij}^2$$

The corresponding (right) eigenvectors are  $R_{ij}^{(1)p} = (1, \lambda_{ij}^{(1)p}/\beta^2)^T$  and  $R_{ij}^{(2)p} = (1, \lambda_{ij}^{(2)p}/\beta^2)^T$ . The upwind term in (31) can then be expressed as:

$$P_{ij}^{-1} |P_{ij}\tilde{A}_{ij}| \Delta^{ij}W = \sum_{k=1}^2 c_k^p(\Delta^{ij}W) | \lambda_{ij}^{(k)p} | \left( P_{ij}^{-1} R_{ij}^{(k)p} \right)$$

where  $c_k^p(\bar{v})$  is the  $k$ -th coordinate of  $\bar{v} \in \mathbb{R}^2$  in the (new) basis formed by the eigenvectors. Once the following entities have been defined:  $r_{ij} = \lambda_{ij}^{(1)p} - \tilde{u}_{ij}\beta^2$ ,  $s_{ij} = \lambda_{ij}^{(2)p} - \tilde{u}_{ij}\beta^2$  (notice that  $r_{ij}s_{ij} = -\tilde{u}_{ij}^2\beta^2$ ), the following relations may be derived:

$$\begin{cases} c_1^p(\Delta^{ij}W) = \frac{1}{2\sqrt{X_{ij}}} ((-s_{ij})\Delta^{ij}\rho + \beta^2\tilde{\rho}_{ij}\Delta^{ij}u) = \frac{\beta^2}{2\sqrt{X_{ij}}} \left( \frac{\Delta^{ij}p}{r_{ij}} + \tilde{\rho}_{ij}\Delta^{ij}u \right) \\ c_2^p(\Delta^{ij}W) = \frac{1}{2\sqrt{X_{ij}}} ((r_{ij})\Delta^{ij}\rho - \beta^2\tilde{\rho}_{ij}\Delta^{ij}u) = \frac{\beta^2}{2\sqrt{X_{ij}}} \left( \frac{\Delta^{ij}p}{-s_{ij}} - \tilde{\rho}_{ij}\Delta^{ij}u \right) \\ P_{ij}^{-1} R_{ij}^{(1)p} = \frac{1}{\beta^2} \left( \begin{array}{c} 1 \\ \tilde{u}_{ij} + r_{ij} \end{array} \right) = \frac{1}{\beta^2} \left( \begin{array}{c} 1 \\ \lambda_{ij}^{(1)p} + \tilde{u}_{ij}(1 - \beta^2) \end{array} \right) \\ P_{ij}^{-1} R_{ij}^{(2)p} = \frac{1}{\beta^2} \left( \begin{array}{c} 1 \\ \tilde{u}_{ij} + s_{ij} \end{array} \right) = \frac{1}{\beta^2} \left( \begin{array}{c} 1 \\ \lambda_{ij}^{(2)p} + \tilde{u}_{ij}(1 - \beta^2) \end{array} \right) \end{cases}$$

Hence:

$$P_{ij}^{-1} |P_{ij}\tilde{A}_{ij}| \Delta^{ij}W = \frac{1}{2\sqrt{X_{ij}}} U_{ij}^p \begin{pmatrix} \Delta^{ij}p \\ \tilde{\rho}_{ij}\Delta^{ij}u \end{pmatrix}$$

where:

$$U_{ij}^p = \begin{pmatrix} U_{ij}^p(1, 1) & U_{ij}^p(1, 2) \\ U_{ij}^p(2, 1) & U_{ij}^p(2, 2) \end{pmatrix} \quad (33)$$

and:

$$\begin{cases} U_{ij}^p(1, 1) = \frac{|\lambda_{ij}^{(1)p}|}{r_{ij}} + \frac{|\lambda_{ij}^{(2)p}|}{-s_{ij}} \\ U_{ij}^p(1, 2) = |\lambda_{ij}^{(1)p}| - |\lambda_{ij}^{(2)p}| \\ U_{ij}^p(2, 1) = \frac{\lambda_{ij}^{(1)p} |\lambda_{ij}^{(1)p}|}{r_{ij}} + \frac{\lambda_{ij}^{(2)p} |\lambda_{ij}^{(2)p}|}{-s_{ij}} + \tilde{u}_{ij}(1 - \beta^2) U_{ij}^p(1, 1) \\ U_{ij}^p(2, 2) = \lambda_{ij}^{(1)p} |\lambda_{ij}^{(1)p}| - \lambda_{ij}^{(2)p} |\lambda_{ij}^{(2)p}| + \tilde{u}_{ij}(1 - \beta^2) U_{ij}^p(1, 2) \end{cases}$$

By substituting the relevant terms into Eq.(12), the new semi-discrete equations finally write:

$$2\delta_i \frac{d}{dt} \begin{pmatrix} \rho_i \\ \rho_i u_i \end{pmatrix} = \begin{pmatrix} \rho_{i-1} u_{i-1} \\ \rho_{i-1} u_{i-1}^2 + p_{i-1} \end{pmatrix} - \begin{pmatrix} \rho_{i+1} u_{i+1} \\ \rho_{i+1} u_{i+1}^2 + p_{i+1} \end{pmatrix} + \frac{1}{2\sqrt{X_{i(i+1)}}} U_{i(i+1)}^p \begin{pmatrix} \Delta^{(i+1)} p \\ \tilde{\rho}_{i(i+1)} \Delta^{(i+1)} u \end{pmatrix} - \frac{1}{2\sqrt{X_{(i-1)i}}} U_{(i-1)i}^p \begin{pmatrix} \Delta^{(i-1)i} p \\ \tilde{\rho}_{(i-1)i} \Delta^{(i-1)i} u \end{pmatrix} \quad (34)$$

### 5.3 Low Mach number limit of the preconditioned semi-discrete equations

By following the same procedure as in Sec. 4.4, we specialize Eq. (34) for  $M_* \rightarrow 0$ . In this limit,  $|\lambda_{ij}^{(1)p}| = \lambda_{ij}^{(1)p}$ ,  $|\lambda_{ij}^{(2)p}| = -\lambda_{ij}^{(2)p}$  and (33) becomes:

$$U_{ij}^p = 2 \begin{pmatrix} 2 + (\beta^2 - 1) \frac{\tilde{u}_{ij}^2}{\tilde{a}_{ij}^2} & (1 + \beta^2) \tilde{u}_{ij} \\ \left( 3 + \beta^2 + (\beta^2 - 1) \frac{\tilde{u}_{ij}^2}{\tilde{a}_{ij}^2} \right) \tilde{u}_{ij} & 2(\tilde{u}_{ij}^2 + \beta^2 \tilde{a}_{ij}^2) \end{pmatrix} \quad (35)$$

By substituting (35) into (34), the following semi-discrete equations are obtained:

$$\begin{aligned} 2\delta_i \frac{d\rho_i}{dt} &= (\rho_{i-1} u_{i-1} - \rho_{i+1} u_{i+1}) \\ &+ \frac{\beta^2 + 1}{2} \left( \frac{\tilde{u}_{i(i+1)}}{\sqrt{X_{i(i+1)}}} \tilde{u}_{i(i+1)} \tilde{\rho}_{i(i+1)} \Delta^{(i+1)} u - \frac{\tilde{u}_{(i-1)i}}{\sqrt{X_{(i-1)i}}} \tilde{\rho}_{(i-1)i} \Delta^{(i-1)i} u \right) \\ &+ \frac{(\beta^2 - 1)}{2} \left( \frac{\tilde{u}_{i(i+1)}^2}{\tilde{a}_{i(i+1)}^2} \frac{\Delta^{(i+1)} p}{\sqrt{X_{i(i+1)}}} - \frac{\tilde{u}_{(i-1)i}^2}{\tilde{a}_{(i-1)i}^2} \frac{\Delta^{(i-1)i} p}{\sqrt{X_{(i-1)i}}} \right) \\ &+ \left( \frac{\Delta^{(i+1)} p}{\sqrt{X_{i(i+1)}}} - \frac{\Delta^{(i-1)i} p}{\sqrt{X_{(i-1)i}}} \right) \end{aligned} \quad (36)$$

$$\begin{aligned}
2\delta_i \frac{d(\rho_i u_i)}{dt} = & (\rho_{i-1} u_{i-1}^2 - \rho_{i+1} u_{i+1}^2) + (p_{i-1} - p_{i+1}) \\
& + \left( \frac{\tilde{u}_{i(i+1)}}{\sqrt{X_{i(i+1)}}} \tilde{u}_{i(i+1)} \tilde{\rho}_{i(i+1)} \Delta^{i(i+1)} u - \frac{\tilde{u}_{(i-1)i}}{\sqrt{X_{(i-1)i}}} \tilde{u}_{(i-1)i} \tilde{\rho}_{(i-1)i} \Delta^{(i-1)i} u \right) \\
& + \frac{\beta^2 - 1}{2} \left( \frac{\tilde{u}_{i(i+1)}^2}{\tilde{a}_{i(i+1)}^2} \frac{\tilde{u}_{i(i+1)}}{\sqrt{X_{i(i+1)}}} \Delta^{i(i+1)} p - \frac{\tilde{u}_{(i-1)i}^2}{\tilde{a}_{(i-1)i}^2} \frac{\tilde{u}_{(i-1)i}}{\sqrt{X_{(i-1)i}}} \Delta^{(i-1)i} p \right) \\
& + \frac{\beta^2 + 3}{2} \left( \frac{\tilde{u}_{i(i+1)}}{\sqrt{X_{i(i+1)}}} \Delta^{i(i+1)} p - \frac{\tilde{u}_{(i-1)i}}{\sqrt{X_{(i-1)i}}} \Delta^{(i-1)i} p \right) \\
& + \beta^2 \left( \frac{\tilde{a}_{i(i+1)}}{\sqrt{X_{i(i+1)}}} \tilde{a}_{i(i+1)} \tilde{\rho}_{i(i+1)} \Delta^{i(i+1)} u - \frac{\tilde{a}_{(i-1)i}}{\sqrt{X_{(i-1)i}}} \tilde{a}_{(i-1)i} \tilde{\rho}_{(i-1)i} \Delta^{(i-1)i} u \right)
\end{aligned} \tag{37}$$

Eqs. (36) and (37) are then non-dimensionalised by using the same reference quantities as in Sec. 4.2 and Sec. 4.4. In the present case, it is necessary to non-dimensionalise also  $X_{ij}$ . By noting that:  $\lim_{\beta^2 \rightarrow 1} X_{ij} = \tilde{a}_{ij}^2$  we choose  $a_\star^2$  as a proper reference quantity and define:

$$X_{ij} = a_\star^2 Y_{ij} = a_\star^2 \left( \left( \frac{1 - \beta^2}{2} \right)^2 \tilde{u}'_{ij}^2 M_\star^2 + \beta^2 \tilde{a}'_{ij}^2 \right)$$

The resulting non-dimensional semi-discrete equations are (the prime is dropped for the sake of clarity):

$$\begin{aligned}
2\delta_i \frac{d\rho_i}{dt} = & (\rho_{i-1} u_{i-1} - \rho_{i+1} u_{i+1}) \\
& + M_\star \frac{\beta^2 + 1}{2} \left( \frac{\tilde{u}_{i(i+1)}}{\sqrt{Y_{i(i+1)}}} \tilde{u}_{i(i+1)} \tilde{\rho}_{i(i+1)} \Delta^{i(i+1)} u - \frac{\tilde{u}_{(i-1)i}}{\sqrt{Y_{(i-1)i}}} \tilde{\rho}_{(i-1)i} \Delta^{(i-1)i} u \right) \\
& + M_\star \frac{(\beta^2 - 1)}{2} \left( \frac{\tilde{u}_{i(i+1)}^2}{\tilde{a}_{i(i+1)}^2} \frac{\Delta^{i(i+1)} p}{\sqrt{Y_{i(i+1)}}} - \frac{\tilde{u}_{(i-1)i}^2}{\tilde{a}_{(i-1)i}^2} \frac{\Delta^{(i-1)i} p}{\sqrt{Y_{(i-1)i}}} \right) \\
& + \frac{1}{M_\star} \left( \frac{\Delta^{i(i+1)} p}{\sqrt{Y_{i(i+1)}}} - \frac{\Delta^{(i-1)i} p}{\sqrt{Y_{(i-1)i}}} \right)
\end{aligned} \tag{38}$$

$$\begin{aligned}
2\delta_i \frac{d(\rho_i u_i)}{dt} &= (\rho_{i-1} u_{i-1}^2 - \rho_{i+1} u_{i+1}^2) + \frac{1}{M_\star^2} (p_{i-1} - p_{i+1}) \\
&+ M_\star \left( \frac{\tilde{u}_{i(i+1)}}{\sqrt{Y_{i(i+1)}}} \tilde{u}_{i(i+1)} \tilde{\rho}_{i(i+1)} \Delta^{i(i+1)} u - \frac{\tilde{u}_{(i-1)i}}{\sqrt{Y_{(i-1)i}}} \tilde{u}_{(i-1)i} \tilde{\rho}_{(i-1)i} \Delta^{(i-1)i} u \right) \\
&+ M_\star \frac{\beta^2 - 1}{2} \left( \frac{\tilde{u}_{i(i+1)}^2}{\tilde{a}_{i(i+1)}^2} \frac{\tilde{u}_{i(i+1)}}{\sqrt{Y_{i(i+1)}}} \Delta^{i(i+1)} p - \frac{\tilde{u}_{(i-1)i}^2}{\tilde{a}_{(i-1)i}^2} \frac{\tilde{u}_{(i-1)i}}{\sqrt{Y_{(i-1)i}}} \Delta^{(i-1)i} p \right) \quad (39) \\
&+ \frac{1}{M_\star} \frac{\beta^2 + 3}{2} \left( \frac{\tilde{u}_{i(i+1)}}{\sqrt{Y_{i(i+1)}}} \Delta^{i(i+1)} p - \frac{\tilde{u}_{(i-1)i}}{\sqrt{Y_{(i-1)i}}} \Delta^{(i-1)i} p \right) \\
&+ \frac{1}{M_\star} \beta^2 \left( \frac{\tilde{a}_{i(i+1)}}{\sqrt{Y_{i(i+1)}}} \tilde{a}_{i(i+1)} \tilde{\rho}_{i(i+1)} \Delta^{i(i+1)} u - \frac{\tilde{a}_{(i-1)i}}{\sqrt{Y_{(i-1)i}}} \tilde{a}_{(i-1)i} \tilde{\rho}_{(i-1)i} \Delta^{(i-1)i} u \right)
\end{aligned}$$

By following the usual procedure, we look for discrete solutions to Eqs.(38) and (39) of the form of (26). In addition we assume that the parameter  $\beta$  is proportional to the reference Mach number, i.e.:

$$\beta = \beta_{ref} M_\star \quad (40)$$

where  $\beta_{ref}$  is a given constant. It should be noted that (40) does not change the minimum power of  $M_\star$  in the semi-discrete equations (which is still  $M_\star^{-2}$ ).

**Note 7** By taking into account (40), it is possible to expand  $Y_{ij}$  as follows:

$$Y_{ij} = M_\star^2 (Y_{2ij} + M_\star Y_{3ij} + \dots)$$

where:

$$\begin{cases} Y_{2ij} = \beta_{ref}^2 \tilde{a}_{0ij}^2 + \frac{1}{4} \tilde{u}_{0ij}^2 \\ Y_{3ij} = 2\beta_{ref}^2 \tilde{a}_{0ij} \tilde{a}_{1ij} + \frac{1}{2} \tilde{u}_{0ij} \tilde{u}_{1ij} \end{cases}$$

As a consequence,  $Y_{ij}^{-1}$  may be expanded as follows:

$$\frac{1}{\sqrt{Y_{ij}}} = \frac{1}{M_\star} \frac{1}{\sqrt{Y_{2ij}}} \left( 1 + \frac{Y_{3ij}}{Y_{2ij}} M_\star + \dots \right)^{-\frac{1}{2}} = \frac{1}{M_\star} \frac{1}{\sqrt{Y_{2ij}}} \left( 1 - \frac{1}{2} \frac{Y_{3ij}}{Y_{2ij}} M_\star + \dots \right)$$

Once the expansions have been introduced into Eqs. (38) and (39), all the terms associated with  $M_\star^{-2}$  and  $M_\star^{-1}$  must be set to zero in order to find the asymptotic solution. The resulting equations are:

1. order  $M_\star^{-2}$  (mass):

$$\frac{\Delta^{i(i+1)} p_0}{\sqrt{Y_{2i(i+1)}}} - \frac{\Delta^{(i-1)i} p_0}{\sqrt{Y_{2(i-1)i}}} = 0 \quad (41)$$

2. order  $M_\star^{-2}$  (momentum):

$$\begin{aligned} & (\Delta^{i(i+1)} p_0 - \Delta^{(i-1)i} p_0) \\ & + \frac{3}{2} \left( \frac{\tilde{u}_{0i(i+1)}}{\sqrt{Y_{2i(i+1)}}} \Delta^{i(i+1)} p_0 - \frac{\tilde{u}_{0(i-1)i}}{\sqrt{Y_{2(i-1)i}}} \Delta^{(i-1)i} p_0 \right) = 0 \end{aligned} \quad (42)$$

3. order  $M_\star^{-1}$  (mass):

$$\begin{aligned} & \left( \frac{\Delta^{i(i+1)} p_1}{\sqrt{Y_{2i(i+1)}}} - \frac{\Delta^{(i-1)i} p_1}{\sqrt{Y_{2(i-1)i}}} \right) \\ & - \frac{1}{2} \left( \frac{Y_{3i(i+1)}}{Y_{2i(i+1)}} \Delta^{i(i+1)} p_0 - \frac{Y_{3(i-1)i}}{Y_{2(i-1)i}} \Delta^{(i-1)i} p_0 \right) = 0 \end{aligned} \quad (43)$$

4. order  $M_\star^{-1}$  (momentum):

$$\begin{aligned} & (\Delta^{i(i+1)} p_1 - \Delta^{(i-1)i} p_1) \\ & + \frac{3}{2} \left( \frac{\tilde{u}_{0i(i+1)}}{\sqrt{Y_{2i(i+1)}}} \Delta^{i(i+1)} p_1 - \frac{\tilde{u}_{0(i-1)i}}{\sqrt{Y_{2(i-1)i}}} \Delta^{(i-1)i} p_1 \right) \\ & + \frac{3}{2} \left( \frac{\tilde{u}_{1i(i+1)}}{\sqrt{Y_{2i(i+1)}}} \Delta^{i(i+1)} p_0 - \frac{\tilde{u}_{1(i-1)i}}{\sqrt{Y_{2(i-1)i}}} \Delta^{(i-1)i} p_0 \right) \\ & - \frac{3}{4} \left( \tilde{u}_{0i(i+1)} \frac{Y_{3i(i+1)}}{Y_{2i(i+1)}} \Delta^{i(i+1)} p_0 - \tilde{u}_{0(i-1)i} \frac{Y_{3(i-1)i}}{Y_{2(i-1)i}} \Delta^{(i-1)i} p_0 \right) = 0 \end{aligned} \quad (44)$$

Eqs. (41) and (42) constitute a system of two homogeneous difference equations for the two unknowns  $\Delta^{(i-1)i} p_0$  and  $\Delta^{i(i+1)} p_0$ . Since the coefficients are obviously arbitrary (depending on the velocity field), it is necessary that:

$$\Delta^{ij} p_0 = 0 \quad \forall(i, j) \quad (45)$$

Therefore  $p_{0i}$  is independent of the index  $i$ :  $p_{0i}(t) = p_0(t)$ . In addition, by exploiting (45), Eqs. (43) and (44) become formally identical to Eqs. (41) and (42) respectively, once  $\Delta^{ij} p_0$  has been replaced with  $\Delta^{ij} p_1$ . Therefore, we can apply to  $p_1$  the same conclusions which

have been reached for  $p_0$ :  $p_{1i}(t) = p_1(t)$ . As a conclusion, when  $M_\star \rightarrow 0$  the pressure solution to Eqs. (38) and (39) is of the form:

$$p_i(t) = p_0(t) + M_\star p_1(t) + M_\star^2 \hat{p}_{2i}(t) \quad (46)$$

By comparing (46) with (19) it is clear that, from a qualitative point of view, the solution associated with the modified numerical scheme exhibit a behavior which is similar to that of the continuous one. This, in principle, should result in a more accurate numerical solution, as confirmed by the numerical experiments reported in Sec. 7.

By virtue of this result, the matrix  $P_{ij}$  which has been used to define the modified numerical flux function (32) can be regarded to as a preconditioner.

## 6 Implicit linearised scheme

### 6.1 Introduction

In this section we propose an implicit algorithm which can be used in order to advance in time the semi-discrete problem defined in Eq. (4). To this purpose, we introduce the following additional definitions:

- $W_i^n = W_i(t = t^n)$ ,  $\Phi_{ij}^n = \Phi_{ij}(t = t^n)$  where  $t^n = n\Delta t$ ;
- $\Delta^n W_i = W_i^{n+1} - W_i^n$  and  $\Delta^n \Phi_{ij} = \Phi_{ij}^{n+1} - \Phi_{ij}^n$ ;
- for any  $G = G(W_i, W_j)$ ,

$$\left\{ \begin{array}{l} \Delta_i G = G(W_i^{n+1}, W_j^n) - G(W_i^n, W_j^n) \\ \Delta_j G = G(W_i^n, W_j^{n+1}) - G(W_i^n, W_j^n) \\ \bar{\Delta}_i G = G(W_i^n, W_j^{n+1}) - G(W_i^{n+1}, W_j^{n+1}) \\ \bar{\Delta}_j G = G(W_i^{n+1}, W_j^n) - G(W_i^{n+1}, W_j^{n+1}) \end{array} \right.$$

In addition, we recall the following property of the Roe flux function. From Sec. 3.1 we know that:  $\tilde{A} = T \text{Diag}(\lambda_1, \lambda_2) T^{-1}$  and  $|\tilde{A}| = T \text{Diag}(|\lambda_1|, |\lambda_2|) T^{-1}$ , where  $\lambda_1, \lambda_2$  are the eigenvalues of  $\tilde{A}$  and  $T$  is the similarity matrix. By introducing:

$$\lambda_k^+ = \max(\lambda_k, 0) \quad \lambda_k^- = \min(\lambda_k, 0) \quad k = 1, 2$$

it is possible to define:

$$\tilde{A}^+ = T \text{Diag}(\lambda_1^+, \lambda_2^+) T^{-1} \quad \tilde{A}^- = T \text{Diag}(\lambda_1^-, \lambda_2^-) T^{-1}$$

Notice that  $\tilde{A}^+ = \tilde{A}^+(W_l, W_r)$  and  $\tilde{A}^- = \tilde{A}^-(W_l, W_r)$ , like  $\tilde{A}$  and  $|\tilde{A}|$ . Furthermore, the following relations hold:

$$\begin{cases} \tilde{A}^+ + \tilde{A}^- = \tilde{A} \\ \tilde{A}^+ - \tilde{A}^- = |\tilde{A}| \end{cases} \quad (47)$$

Eq. (47), together with property 3 in Sec. 3.1, permit to recast the Roe flux function as follows:

$$\begin{aligned} \Phi_{lr} &= \frac{F(W_l) + F(W_r)}{2} - \frac{1}{2}|\tilde{A}(W_l, W_r)|(W_r - W_l) \\ &= F(W_l) + \tilde{A}^-(W_l, W_r)(W_r - W_l) \\ &= F(W_r) - \tilde{A}^+(W_l, W_r)(W_r - W_l) \end{aligned} \quad (48)$$

## 6.2 The non-preconditioned case

The following implicit (backward Euler) scheme is firstly considered:

$$\frac{\delta_i}{\Delta t} \Delta^n W_i + \Phi_{i(i+1)}^{n+1} - \Phi_{(i-1)i}^{n+1} = 0 \quad (49)$$

where  $\Phi_{ij}$  is given by (13). Eq.(49) can be recast as follows:

$$\frac{\delta_i}{\Delta t} \Delta^n W_i + \Delta^n \Phi_{i(i+1)} - \Delta^n \Phi_{(i-1)i} = -(\Phi_{i(i+1)}^n - \Phi_{(i-1)i}^n) \quad (50)$$

Let us assume that there exist two matrices:

$$H_{ij}^{(1)n} = H^{(1)}(W_i^n, W_j^n) \quad H_{ij}^{(2)n} = H^{(2)}(W_i^n, W_j^n)$$

such that:

$$\Delta^n \Phi_{ij} \simeq H_{ij}^{(1)n} \Delta^n W_i + H_{ij}^{(2)n} \Delta^n W_j \quad (51)$$

Then, substituting the approximation of  $\Delta^n \Phi_{ij}$  (51) into Eq.(50) the following scheme is obtained:

$$\begin{aligned} -H_{(i-1)i}^{(1)n} \Delta^n W_{i-1} + \left( \frac{\delta_i}{\Delta t} I + H_{i(i+1)}^{(1)n} - H_{(i-1)i}^{(2)n} \right) \Delta^n W_i \\ + H_{i(i+1)}^{(2)n} \Delta^n W_{i+1} = -(\Phi_{i(i+1)}^n - \Phi_{(i-1)i}^n) \end{aligned} \quad (52)$$

where  $I$  is the identity matrix. Eq.(52) represents a block tridiagonal linear system for the unknowns:  $\Delta^n W_{i-1}$ ,  $\Delta^n W_i$  and  $\Delta^n W_{i+1}$ . Once it has been solved, the unknowns at time  $t^{n+1}$  are directly given by:  $W_i^{n+1} = W_i^n + \Delta^n W_i, \forall i$ . Therefore, under the basic assumption (51), the original non-linear scheme (i.e. Eq.(49)) has been linearised.

**Note 8** If the numerical flux function was differentiable, (51) could be regarded to as a first-order Taylor expansion with respect to  $t$ , i.e. a linearisation in time. In such a case,  $H_{ij}^{(1)} = \partial\Phi_{ij}/\partial W_i$  and  $H_{ij}^{(2)} = \partial\Phi_{ij}/\partial W_j$ . However, the Roe flux function is not differentiable and (51) must be introduced as an additional requirement on the existence of  $H_{ij}^{(1)}$  and  $H_{ij}^{(2)}$ .

**Note 9** If the numerical flux function was first-order homogeneous (as for the case of the Euler equations associated with an ideal polytropic state equation, see Note 2), it would be possible to express the flux function as follows:

$$\Phi(W_l, W_r) = \bar{H}^{(1)}(W_l, W_r) W_l + \bar{H}^{(2)}(W_l, W_r) W_r \quad (53)$$

By assuming  $\bar{H}^{(1)}$  and  $\bar{H}^{(2)}$  to be weakly dependent on  $(W_l, W_r)$ , it is then possible to approximate  $\Delta^n \Phi_{ij}$  as in (51). This is a rather classical approach to obtain a linearised implicit scheme like (52) (see [4]).

However, we want to point out here that, in the case of the Roe flux function, there is not unicity of  $(\bar{H}^{(1)}, \bar{H}^{(2)})$  which satisfies Eq. (53). Indeed, by virtue of Eq.(48) and of the flux first-order homogeneity, the couple  $(\bar{H}^{(1)}, \bar{H}^{(2)})$  can be expressed at least in three different ways:

$$\begin{cases} \bar{H}_a^{(1)} = \frac{1}{2} \left( A(W_l) + |\tilde{A}(W_l, W_r)| \right) & \bar{H}_a^{(2)} = \frac{1}{2} \left( A(W_r) - |\tilde{A}(W_l, W_r)| \right) \\ \bar{H}_b^{(1)} = \tilde{A}^+(W_l, W_r) & \bar{H}_b^{(2)} = A(W_r) - \tilde{A}^+(W_l, W_r) \\ \bar{H}_c^{(1)} = A(W_l) - \tilde{A}^-(W_l, W_r) & \bar{H}_c^{(2)} = \tilde{A}^-(W_l, W_r) \end{cases}$$

Thus, a class of admissible numerical schemes can be defined by taking into Eq. (52)  $H_{lr}^{(k)n}$  defined by:

$$H_{lr}^{(k)n} = \bar{H}_{\gamma}^{(k)}(W_l^n, W_r^n) = \gamma \bar{H}_b^{(k)}(W_l^n, W_r^n) + (1 - \gamma) \bar{H}_c^{(k)}(W_l^n, W_r^n) \quad k = 1, 2$$

where  $\gamma$  is a free parameter.

In particular,  $(\bar{H}_a^{(1)}, \bar{H}_a^{(2)})$  corresponds to  $\gamma = \frac{1}{2}$ .

Let us introduce a specific property of the Roe flux function which is valid regardless of the specific state equation (for the proof refer to Sec. B):

**Lemma 2** Any Roe's numerical flux function satisfies the following relation:

$$\Delta^n \Phi_{ij} = \tilde{A}^+(W_i^n, W_j^n) \Delta^n W_i + \tilde{A}^-(W_i^n, W_j^n) \Delta^n W_j + R_{ij}^{n,n+1} \quad (54)$$

where  $R_{ij}^{n,n+1}$  is given by:

$$\begin{aligned} 2R_{ij}^{n,n+1} = & \left( \Delta_i \tilde{A}^+ + \Delta_j \tilde{A}^+ \right) \Delta^n W_i \\ & + \left( \Delta_i \tilde{A}^- + \Delta_j \tilde{A}^- \right) \Delta^n W_j \\ & + \left( \Delta_j \tilde{A}^- - \Delta_i \tilde{A}^+ \right) \Delta^{ij} W^n \\ & + \left( \bar{\Delta}_i \tilde{A}^+ - \bar{\Delta}_j \tilde{A}^- \right) \Delta^{ij} W^{n+1} \end{aligned}$$

Therefore, if it is possible to state that, for all  $(W_i^n, W_j^n, W_i^{n+1}, W_j^{n+1})$  in a same neighbourhood:

$$\| R_{ij}^{n,n+1} \| \ll \| \tilde{A}^+(W_i^n, W_j^n) \Delta^n W_i + \tilde{A}^-(W_i^n, W_j^n) \Delta^n W_j \| \quad (55)$$

for a certain norm  $\|\cdot\|$ , then  $\Delta^n \Phi_{ij}$  can be approximated as follows:

$$\Delta^n \Phi_{ij} \simeq \tilde{A}^+(W_i^n, W_j^n) \Delta^n W_i + \tilde{A}^-(W_i^n, W_j^n) \Delta^n W_j \quad (56)$$

**Note 10** If  $\tilde{A}^+$  and  $\tilde{A}^-$  are independent of  $(W_i^n, W_j^n)$ , since in this case  $R_{ij}^{n,n+1} = 0$ , (55) is trivially satisfied. However, having  $\tilde{A}^+$  and  $\tilde{A}^-$  independent of  $(W_i^n, W_j^n)$  is not a necessary condition. Indeed, for any enough regular function  $G = G(W_i^n, W_j^n) = G(W(x_i, t^n), W(x_j, t^n))$  with  $x_i = i\Delta x$ ,  $t^n = n\Delta t$  and  $\Delta t \rightarrow 0$ , the following relations are verified:

$$\begin{cases} \| \Delta_i G \| \simeq \| \bar{\Delta}_i G \| \simeq \| \Delta^n W_i \| = O(\Delta t) \\ \| \Delta_j G \| \simeq \| \bar{\Delta}_j G \| \simeq \| \Delta^n W_j \| = O(\Delta t) \end{cases} \quad (57)$$

In particular, to have (57), it is sufficient to take  $\tilde{A}^+$  and  $\tilde{A}^-$  Lipschitzian with respect to their arguments. Furthermore, when  $\Delta x$  tends to zero, the following relation is also satisfied:

$$\| \Delta^{ij} W^{n+1} \| \simeq \| \Delta^{ij} W^n \| = O(\Delta x)$$

As a consequence:

$$\| R_{ij}^{n,n+1} \| = O((\Delta t)^2) + O(\Delta t \Delta x)$$

while:

$$\| \tilde{A}^+(W_i^n, W_j^n) \Delta^n W_i + \tilde{A}^-(W_i^n, W_j^n) \Delta^n W_j \| = O(\Delta t)$$

In conclusion, (55) should be locally satisfied in every space-time domain where the numerical flux function is regular enough.

In view of the direct comparison between (56) and (51) we set:

$$\begin{cases} H_{ij}^{(1)n} = \tilde{A}^+(W_i^n, W_j^n) \\ H_{ij}^{(2)n} = \tilde{A}^-(W_i^n, W_j^n) \end{cases}$$

In conclusion, under the validity of the assumption (55), the following scheme can be proposed:

$$B_{-1}^{i,n} \Delta^n W_{i-1} + B_0^{i,n} \Delta^n W_i + B_1^{i,n} \Delta^n W_{i+1} = - (\Phi_{i(i+1)}^n - \Phi_{(i-1)i}^n) \quad (58)$$

in which:

$$\begin{cases} B_{-1}^{i,n} = -\tilde{A}^+(W_{i-1}^n, W_i^n) \\ B_0^{i,n} = \frac{\delta_i}{\Delta t} I + \tilde{A}^+(W_i^n, W_{i+1}^n) - \tilde{A}^-(W_{i-1}^n, W_i^n) \\ B_1^{i,n} = \tilde{A}^-(W_i^n, W_{i+1}^n) \end{cases}$$

**Note 11** It may be worth remarking that the scheme (58) has been derived by exploiting only the algebraic properties of the Roe matrix. Therefore:

- it does not depend on the specific state equation which completes the mathematical problem. Hence, the proposed scheme can be applied to the specific case under consideration, i.e. a Roe's flux function associated with a barotropic fluid;
- it may be directly applied to the complete set of governing equations (including the energy balance).

### 6.3 The preconditioned case

Let us consider the modified flux function introduced in (31):

$$\Phi_{lr} = \frac{F(W_l) + F(W_r)}{2} - \frac{1}{2} P_{lr}^{-1} |P_{lr} \tilde{A}_{lr}| (W_r - W_l)$$

Since:

$$F(W_l) + F(W_r) = \begin{cases} 2F(W_l) + \tilde{A}_{lr} (W_r - W_l) \\ 2F(W_r) - \tilde{A}_{lr} (W_r - W_l) \end{cases}$$

and:

$$P_{lr}^{-1} |P_{lr} \tilde{A}_{lr}| = \begin{cases} 2P_{lr}^{-1} (P_{lr} \tilde{A}_{lr})^+ - \tilde{A}_{lr} \\ \tilde{A}_{lr} - 2P_{lr}^{-1} (P_{lr} \tilde{A}_{lr})^- \end{cases}$$

it is possible to express the preconditioned numerical flux function in three equivalent ways, namely:

$$\begin{aligned}\Phi_{lr} &= \frac{F(W_l) + F(W_r)}{2} - \frac{1}{2} P_{lr}^{-1} |P_{lr} \tilde{A}_{lr}| (W_r - W_l) \\ &= F(W_l) + P_{lr}^{-1} (P_{lr} \tilde{A}_{lr})^- (W_r - W_l) \\ &= F(W_r) - P_{lr}^{-1} (P_{lr} \tilde{A}_{lr})^+ (W_r - W_l)\end{aligned}\quad (59)$$

The formal identity between (59) and (48) is evident. Therefore, once  $(\tilde{A}_{ij}^+, \tilde{A}_{ij}^-)$  has been replaced with  $(P_{ij}^{-1} (P_{ij} \tilde{A}_{ij})^+, P_{ij}^{-1} (P_{ij} \tilde{A}_{ij})^-)$ , it is possible to directly apply Lemma 2 to the preconditioned numerical flux function. As a consequence, by exploiting the same kind of assumptions as for the non-preconditioned case, we can set:

$$\begin{cases} H_{ij}^{(1)n} = (P_{ij}^n)^{-1} (P_{ij}^n \tilde{A}_{ij}^n)^+ \\ H_{ij}^{(2)n} = (P_{ij}^n)^{-1} (P_{ij}^n \tilde{A}_{ij}^n)^- \end{cases}$$

where  $P_{ij}^n = P_{ij}(W_i^n, W_j^n)$  and  $\tilde{A}_{ij}^n = \tilde{A}_{ij}(W_i^n, W_j^n)$ . In conclusion, the following scheme can be proposed for the preconditioned case:

$$C_{-1}^{i,n} \Delta^n W_{i-1} + C_0^{i,n} \Delta^n W_i + C_1^{i,n} \Delta^n W_{i+1} = - (\Phi_{i(i+1)}^n - \Phi_{(i-1)i}^n) \quad (60)$$

where:

$$\begin{cases} C_{-1}^{i,n} = - (P_{i-1,i}^n)^{-1} (P_{i-1,i}^n \tilde{A}_{i-1,i}^n)^+ \\ C_0^{i,n} = \frac{\delta_i}{\Delta t} I + (P_{i,i+1}^n)^{-1} (P_{i,i+1}^n \tilde{A}_{i,i+1}^n)^+ - (P_{i-1,i}^n)^{-1} (P_{i-1,i}^n \tilde{A}_{i-1,i}^n)^- \\ C_1^{i,n} = (P_{i,i+1}^n)^{-1} (P_{i,i+1}^n \tilde{A}_{i,i+1}^n)^- \end{cases}$$

**Note 12** As for the non-preconditioned case, it may be worth remarking that the scheme (60) has been derived by exploiting only the algebraic properties of the Roe matrix. Therefore:

- it does not depend on the specific state equation which completes the mathematical problem. Hence, the proposed scheme can be applied to the specific case under consideration, i.e. a (preconditioned) Roe flux function associated with a barotropic fluid;
- it may be directly applied to the complete set of governing equations (including the energy balance).

## 7 1D numerical experiments

### 7.1 Description of the problem

The 1D inviscid flow in a nozzle is considered; the governing equations are the following:

$$\frac{\partial W}{\partial t} + \frac{\partial F(W)}{\partial x} = Q \quad (61)$$

where:

$$W = \begin{pmatrix} \rho \\ \rho u \end{pmatrix} \text{ and } F(W) = \begin{pmatrix} \rho u \\ \rho u^2 + p \end{pmatrix}$$

and  $Q$  is a source term, which accounts for variations of the cross-sectional area  $A$  of the nozzle:

$$Q = -\frac{1}{A} \left( \frac{dA}{dx} \right) \begin{pmatrix} \rho u \\ \rho u^2 \end{pmatrix}$$

Since the final aim of the present work is the simulation of cavitating flows typical of aerospace applications, we choose a particular state law. More precisely, we consider a cavitation flow model recently proposed in [3]. As shown in [14], this model seems to be a good compromise between computational cost and physical representativeness (it can account for thermal cavitation effects and the concentration of the active nuclei in the liquid phase). This model leads to the following barotropic state law:

$$p < p_{sat}; \quad \frac{1}{\rho a^2} = \frac{1}{\rho} \frac{dp}{dp} = \frac{1-\alpha}{p} \left[ (1-\varepsilon_l) \frac{p}{\rho_{lsat} a_l^2} + \varepsilon_l g^* \left( \frac{p_c}{p} \right)^\eta \right] + \frac{\alpha}{\gamma_v p} \quad (62)$$

where:

- $\alpha$  is the void fraction defined here as  $\alpha = \frac{\rho}{\rho_{lsat}} - 1$ ;
- $\varepsilon_l$  is a known function of  $\alpha$  and of  $\delta_T/R$ , which is a given input parameter;
- $p_c$ ,  $g^*$ ,  $\eta$ ,  $\gamma_v$  are known constants depending on the considered liquid;
- $\rho_{lsat}$  is the liquid saturation density, depending on the (constant) temperature  $T_\infty$  of the whole flow, which is another input parameter;
- $a_l$  is a known constant representing the liquid sound speed at saturation conditions.

In non cavitating regions ( $p > p_{sat}$ ) the state law for a weakly compressible liquid is adopted:

$$p > p_{sat}; \quad p = p_{sat} + \frac{1}{\beta_{sl}} \ln \left( \frac{\rho}{\rho_{lsat}} \right) \quad (63)$$

where the “isentropic compressibility”  $\beta_{sl}$  is assumed constant, depending on the specific liquid under consideration. Thus, given the density, pressure can be obtained numerically from Eq. (62) and analytically from Eq. (63).

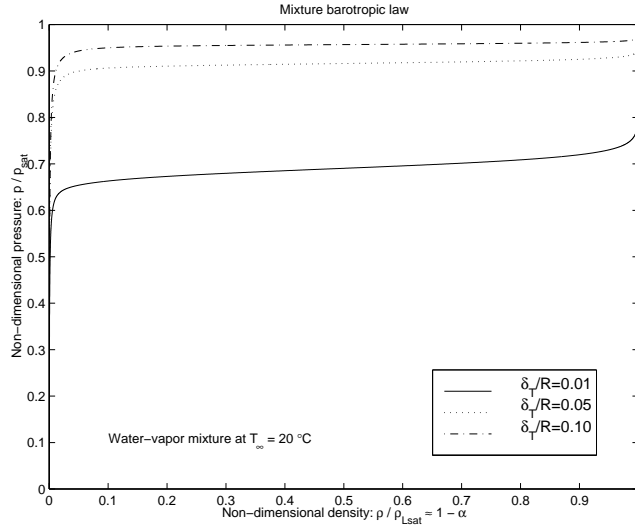


Figure 1: Pressure variation with density for a water-vapor mixture

**Note 13** Within the limits of the chosen model, the whole flow (i.e. the pure liquid and the mixture regions) behave isentropically. Hence,  $a = dp/d\rho$  can be rightfully regarded to as the fluid sound speed and, by virtue of the physical foundation of the model, it is always strictly positive, as assumed in Sec. 2.

Once  $p$  is computed, the sound speed  $a$  is explicitly given by Eq. (62) as a function of  $p$  and  $\rho$ . In practice, the barotropic law is numerically integrated as a pre-processing; a table of discrete values  $(p_i, \rho_i, a_i)$  is thus created. During the simulation, given the value of density, the pressure and the speed of sound are obtained from this table by linear interpolation. Details of the numerical solution of Eq. (62) and of the use of the discrete table can be found in Appendix C, while for details of the cavitation model we refer to [3] and [14].

Besides practical applications, as previously mentioned in the Introduction, the barotropic law in Eq. (62) leads to a challenging problem from a numerical viewpoint. Indeed, the variation of  $p$  with  $\rho$  is very steep especially near the saturation point, as shown, for instance, in Fig. 1 for a water-vapor mixture. Moreover, the Mach number varies of several orders of magnitude between non cavitating and cavitating regions. Indeed, for a water-vapor mixture at  $T_\infty=20^\circ\text{C}$ ,  $a$  can range from 1500 (m/s) in the liquid region to as low as 0.1 (m/s) in the mixture region, as shown in Fig. 2.

In our simulations, the employed liquid is water at  $T_\infty=20^\circ\text{C}$ . The values of the various parameters in Eqs. (62) and (63) are the following:  $\beta_{sl}=5 \cdot 10^{-5}$  (1/Pa),  $p_c=22089000$  (Pa),  $g^*=1.67$ ,  $\eta=0.73$ ,  $\gamma_v=1.28$ ,  $\delta_T/R=0.1$ ,  $p_{\text{sat}}=2339.953$  (Pa),  $\rho_{\text{lsat}}=997.949$  (Kg/m<sup>3</sup>) and  $a_l=1415.7$  (m/s).

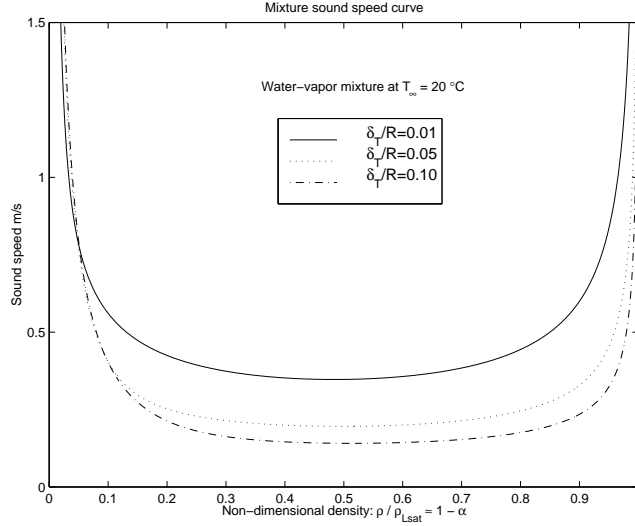


Figure 2: Speed-of-sound variation with density for a water-vapor mixture

A convergent-divergent nozzle of adimensionalised length  $L = 21.4$  is discretised with 360 cells. The cell width is refined by a geometric progression in the convergent part to reach  $\Delta x = 0.02$  at the nozzle throat; in the divergent part the grid is specular. The nozzle geometry and the cell distribution are illustrated in Fig. 3. At the inflow, non-homogeneous Dirichlet conditions are imposed on density and velocity ( $\rho = \rho_{\infty}$ ,  $u = u_{\infty}$ ), while at the outflow homogeneous Neumann conditions are used. These boundary conditions are numerically imposed by Steger-Warming decomposition [15]. Initially, the flow field is assumed uniform at  $\rho = \rho_{\infty}$  and  $u = u_{\infty}$  and  $Q = 0$  (constant section); then  $Q$  is linearly increased to reach its actual value at a non-dimensional time  $\tau = 0.5$ . Time-advancing is carried out either by an explicit 4-step Runge-Kutta scheme or by the implicit algorithm described in Sec. 6. The simulations are advanced in time until a steady state is reached.

Finally, as for the preconditioning strategy proposed in Sec. 5, it is clear that it should be applied only to those regions where the flow is nearly incompressible, i.e. to the pure liquid. Since the liquid fraction of the cavitating mixture is a local variable, the asymptotic analysis of Secs. 4 and 5 cannot be rigorously applied. However, we assume that it is locally applicable at any cell interface where the flow is liquid ( $p \geq p_{\text{sat}}$ ) on both sides. Hence, a first-stage implementation of a local preconditioning strategy can be based on the matrix (32), where  $\beta$  is now a variable defined as follows:

$$\beta(W_l, W_r) = \begin{cases} \beta_{\text{th}} & \text{if } p_l \geq p_{\text{sat}} \text{ and } p_r \geq p_{\text{sat}} \\ 1 & \text{otherwise} \end{cases}$$

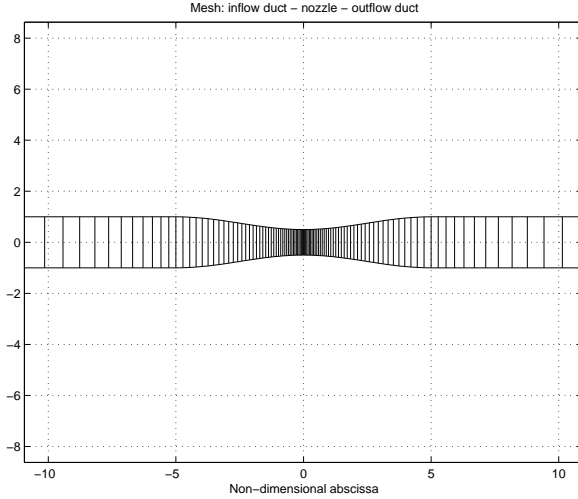


Figure 3: Nozzle geometry and computational cell distribution

where  $\beta_{th}$  is the theoretical value given by (40) and  $M_\star$  is a characteristic Mach number of the liquid region, e.g. the inflow Mach number.

## 7.2 Results and discussion

The various considered conditions are summarized in Tab. 1, in which  $\sigma$  is the cavitation number, defined as follows:

$$\sigma = \frac{p_\infty - p_{sat}}{1/2 \rho_\infty u_\infty}$$

In our simulations, cavitation phenomena occur in test-cases TC8, TC11 and TC13.

First, results obtained without preconditioning and with explicit time advancing are discussed. The anticipated lack of accuracy of the non-preconditioned solution in the incompressible limit (very low Mach numbers) is clearly visible, for instance, in Fig. 4, in which the steady state solution is reported for test-case TC9. Indeed, both density and pressure show an unphysical asymmetric behavior (the minimum should occur at the nozzle throat). The same behavior has been observed in all the considered test-cases; an example for a cavitating flow (TC11) is given in Fig. 5. In this case, the inaccuracy is evident in the behavior of pressure in the convergent part, just before cavitation. In order to obtain a correct solution, the Mach number has to be increased to approximately  $10^{-1}$  (see, for instance, Fig. 6), which corresponds to conditions difficult to be reached for a liquid flow.

Test-case	$p_\infty$ (atm)	$u_\infty$ (m/s)	$M_\infty$	$\sigma$
TC1	10	0.1	$7 \cdot 10^{-5}$	202587
TC2	5	0.1	$7 \cdot 10^{-5}$	101059
TC3	1	0.1	$7 \cdot 10^{-5}$	19837
TC4	0.1	0.1	$7 \cdot 10^{-5}$	1562
TC5	10	1	$7 \cdot 10^{-4}$	2026
TC6	5	1	$7 \cdot 10^{-4}$	1011
TC7	1	1	$7 \cdot 10^{-4}$	199
TC8	0.1	1	$7 \cdot 10^{-4}$	<b>16</b>
TC9	10	5	$3.5 \cdot 10^{-3}$	81
TC10	5	5	$3.5 \cdot 10^{-3}$	40
TC11	1	5	$3.5 \cdot 10^{-3}$	<b>8</b>
TC12	10	10	$7 \cdot 10^{-3}$	20
TC13	5	10	$7 \cdot 10^{-3}$	<b>10</b>

Table 1: Main features of the different considered test-cases

As for time advancing, all simulations are stable at  $\Delta t = 10^{-5}$ ; since the steady state is reached at  $t \simeq 1$ , CPU times (on a PC with 1200Mhz processor and 256Mb RAM) of about 150s and 450s are respectively needed.

The proposed preconditioning technique appears effective in eliminating accuracy problems for all the considered test-cases. This is shown, for instance, in Figs. 7 and 8 for test cases TC9 and TC11 respectively, in which the unphysical behaviors of pressure and density are completely eliminated. This gives an a-posteriori support to the results of the asymptotic analysis and to the proposed formulation. It may be worth remarking that the numerical results also validate the general structure of the preconditioner and, in particular, the assumption (40). Indeed, it should be noted that  $\beta$  in Tab. 2 is derived from  $M_*$  in Tab. 1 by essentially exploiting (40) with  $\beta_{ref} \simeq 45$ . However, the preconditioning procedure dramatically reduces the time step allowed by the stability of the explicit time advancing scheme, especially for the lowest Mach number cases, as shown in Tab. 2. In particular, it is clear from Tab. 2 that preconditioned explicit simulations are hardly affordable in 3D.

The situation is remarkably improved by the proposed implicit time advancing; for the non cavitating test cases, the time step can be increased indefinitely and, hence, the CPU time needed to reach the steady state becomes negligible. As for cavitating flows, for test-cases TC11 and TC13 the  $\Delta t$  can be increased up to  $10^{-5}$  leading to simulations requiring a CPU time of about 120s. Surprisingly, with implicit time-advancing, the simulation of TC8 was not stable; this might be due to the unphysical transient (the variation of  $Q$  in Eq. 61), which implies large oscillations of pressure when cavitation phenomena occur. This inconvenient might be overcome by ad-hoc variable  $\Delta t$ ; however, in our opinion, this is beyond the scope of the present paper.

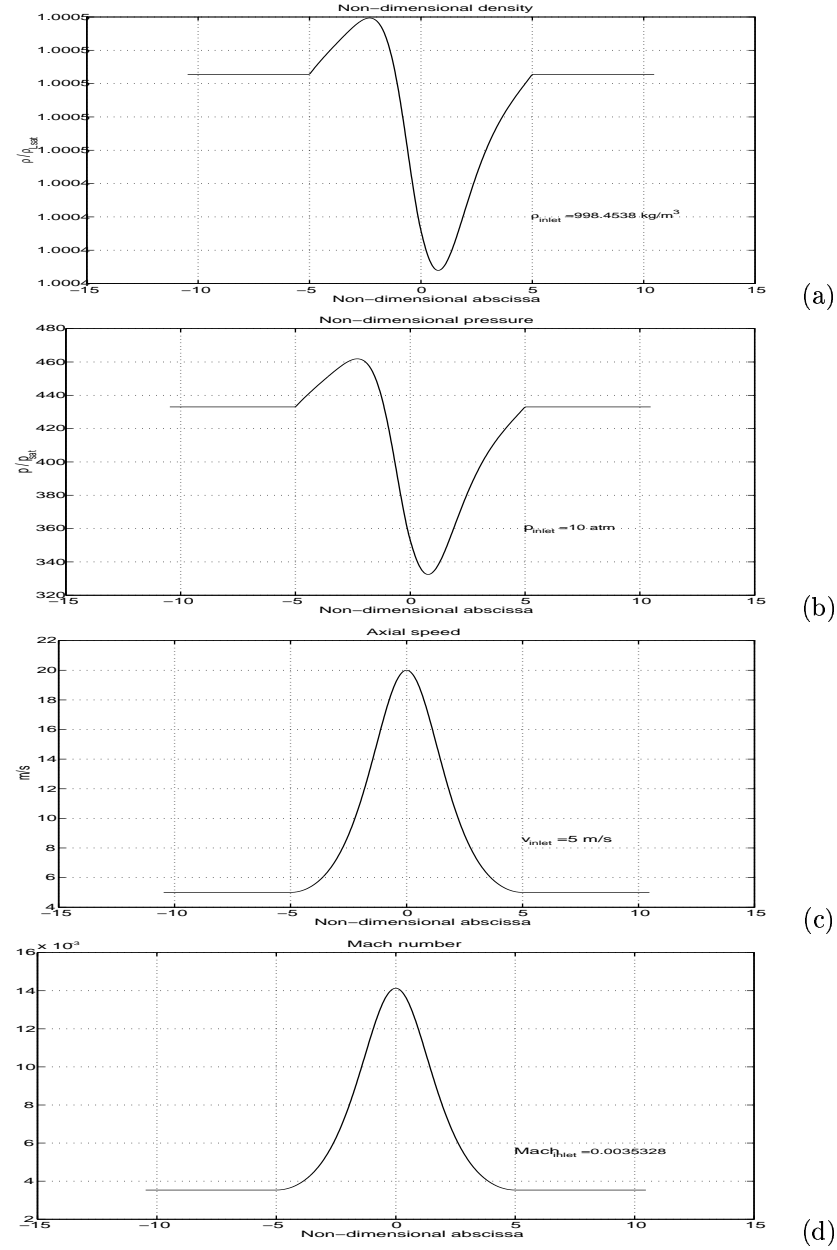


Figure 4: Steady state solution obtained for test case TC9 without preconditioning; a) density; b) pressure; c) axial speed ; d) Mach number.

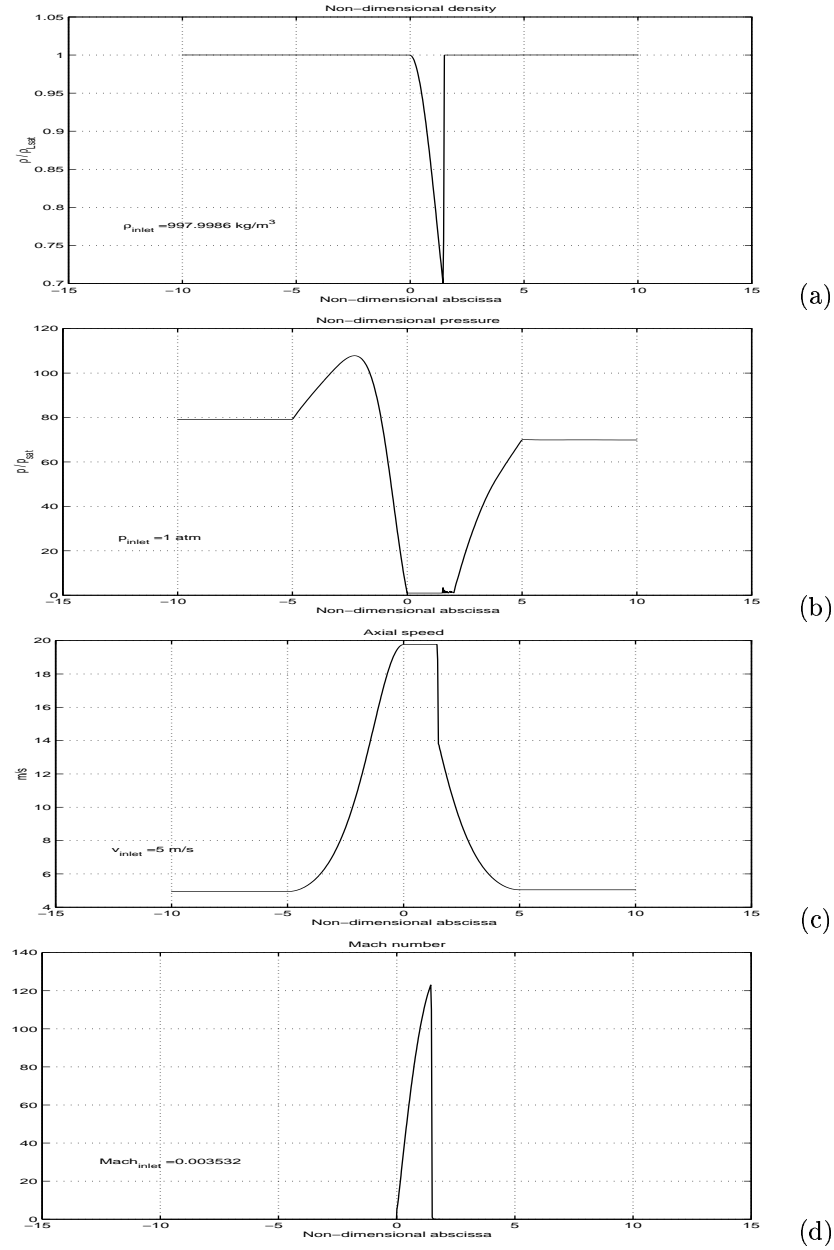


Figure 5: Steady state solution obtained for test case TC11 without preconditioning; a) density; b) pressure; c) axial speed ; d) Mach number.

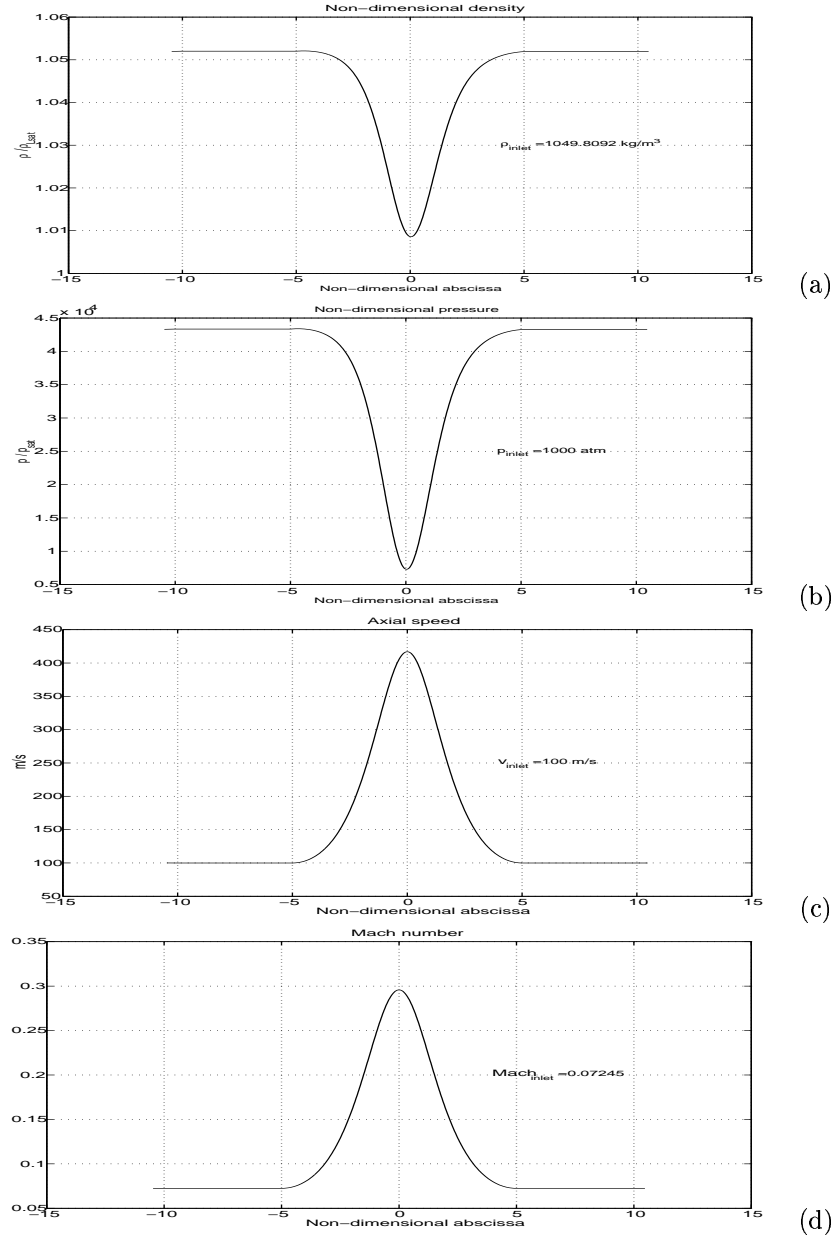


Figure 6: Steady state solution obtained without preconditioning for  $M_\infty = 7 \cdot 10^{-2}$ ; a) density; b) pressure; c) axial speed ; d) Mach number.

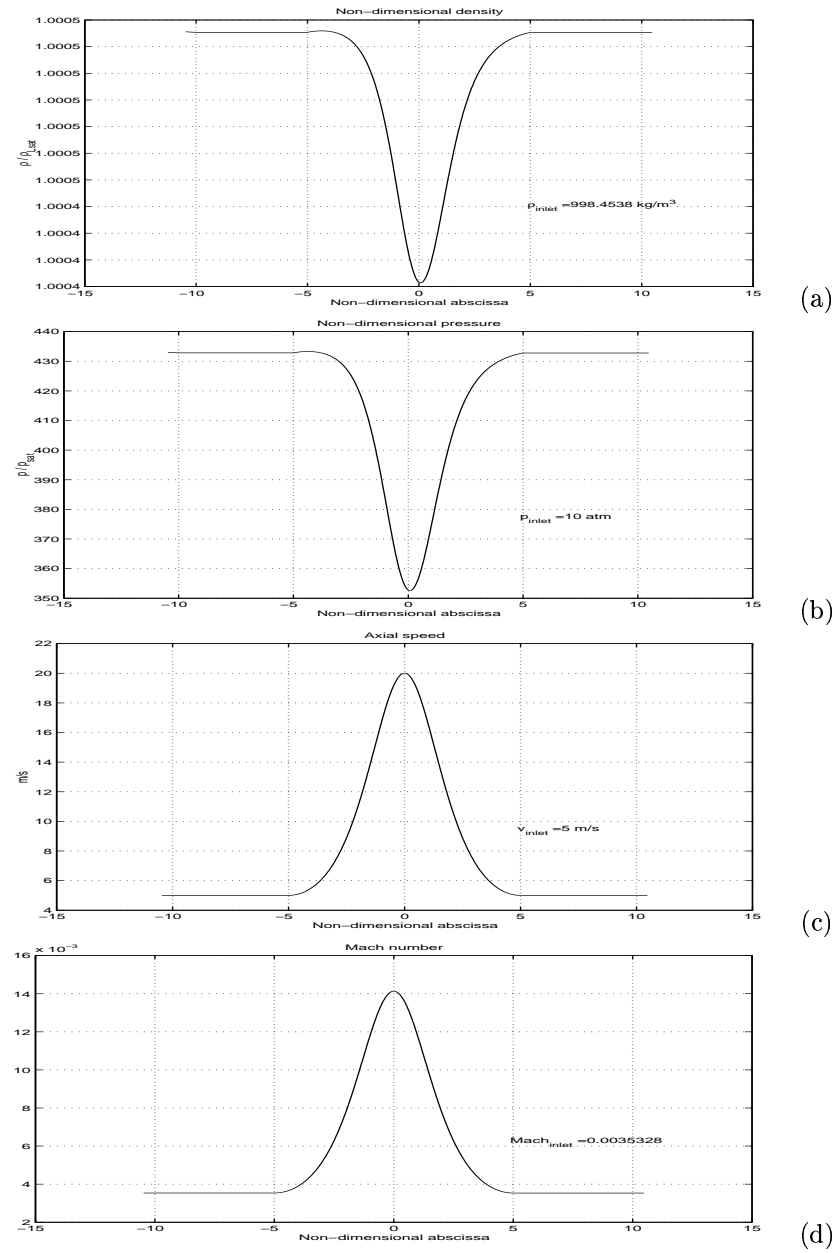


Figure 7: Steady state solution obtained for test case TC9 with preconditioning; a) density; b) pressure; c) axial speed ; d) Mach number.

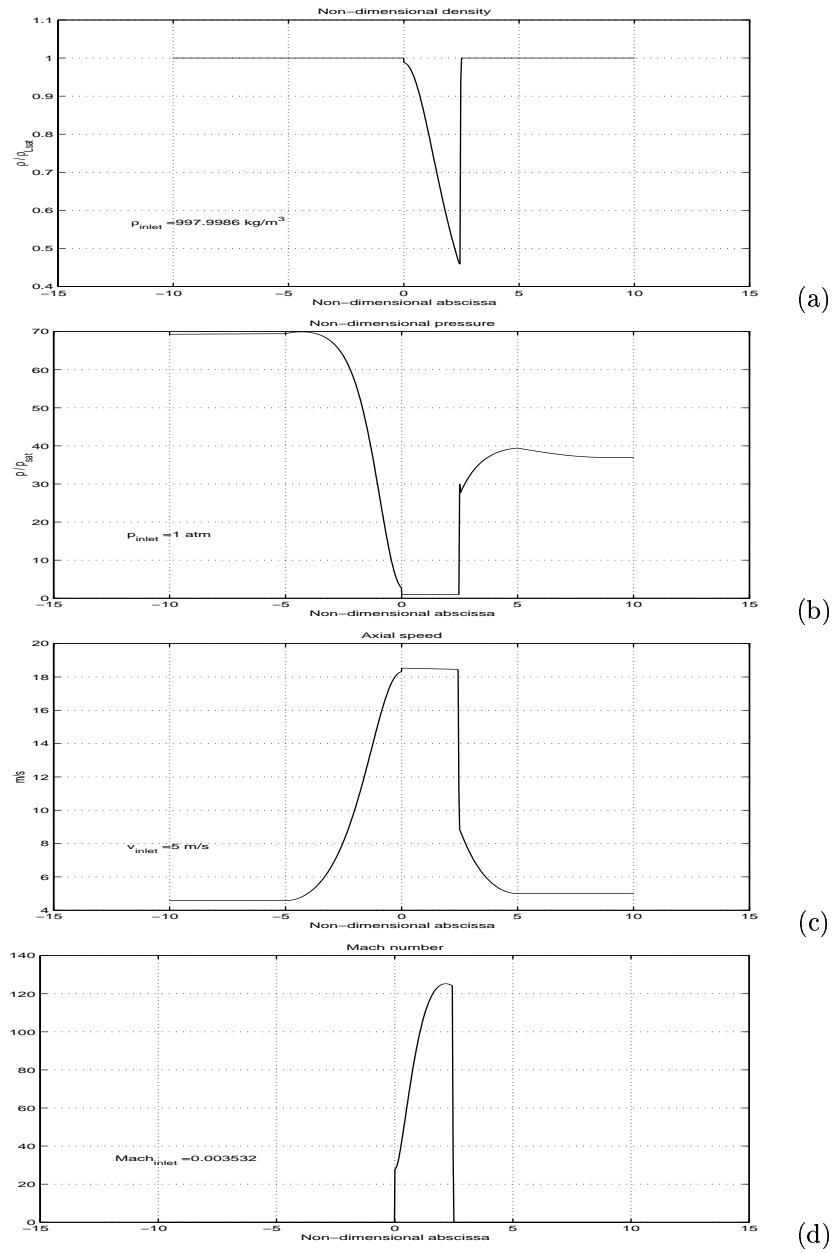


Figure 8: Steady state solution obtained for test case TC11 with preconditioning; a) density; b) pressure; c) axial speed ; d) Mach number.

Test-case	$\beta^2$	$\Delta t$	CPU
TC1	$10^{-5}$	$5 \cdot 10^{-8}$	8h20m
TC2	$10^{-5}$	$5 \cdot 10^{-8}$	8h20m
TC3	$10^{-5}$	$5 \cdot 10^{-8}$	8h20m
TC4	$10^{-5}$	$5 \cdot 10^{-8}$	8h20m
TC5	$10^{-3}$	$5 \cdot 10^{-7}$	50m
TC6	$10^{-3}$	$5 \cdot 10^{-7}$	50m
TC7	$10^{-3}$	$5 \cdot 10^{-7}$	50m
TC8	$10^{-3}$	$10^{-7}$	4h10m
TC9	$10^{-2}$	$10^{-6}$	25m
TC10	$10^{-2}$	$10^{-6}$	25m
TC11	$10^{-2}$	$5 \cdot 10^{-7}$	50m
TC12	$10^{-1}$	$5 \cdot 10^{-6}$	5m
TC13	$10^{-1}$	$5 \cdot 10^{-6}$	5m

Table 2: Parameters of the preconditioned explicit simulations

## 8 Conclusions

The discretisation of the Euler equations for a barotropic state law has been considered. The adaptation of the Roe scheme to the barotropic case has first been presented. Then, an asymptotic study for the incompressible limit has been performed both in the continuous and discrete case, showing that the discrete solution admits pressure oscillations in space much larger than those of the exact one. This is the same kind of behaviour observed in previous studies (e.g. [8] for the case of a polytropic state law). It has been shown that the same kind of preconditioning as in [8] is suitable also for a barotropic flow, in that the preconditioned discrete formulation has an asymptotic behaviour in agreement with the continuous case. Finally, a linearised implicit time-advancing algorithm has been defined using the properties of the Roe matrix, instead of the first-order homogeneity of the flux function, which is not satisfied here. The implicit formulation has also been extended to the preconditioned scheme. Note that the whole numerical framework developed in this study is not specific to cavitation problems: indeed, the preconditioned Roe scheme can be applied to any barotropic flow in presence of high and/or low Mach number. Furthermore, the implicit linearisation can be applied also to non barotropic flows; indeed, this formulation is suitable for any Roe's scheme, for conservative laws with homogeneous as well as non-homogeneous flux functions.

All the proposed numerical ingredients have been applied to a quasi-1D nozzle flow of a cavitating liquid. The homogeneous flow model proposed in [3] has been adopted here, which leads to a barotropic state law in the form of a non-linear differential equation, which is solved numerically as a pre-processing. Besides practical applications, the considered barotropic law leads to a challenging problem from a numerical viewpoint. Indeed, the

variation of  $p$  with  $\rho$  is very steep especially near the saturation point and the Mach number varies of several orders of magnitude between non cavitating and cavitating regions.

The results of the carried-out 1D numerical experiments well illustrate the problems encountered in this type of applications and the effectiveness of the proposed remedies. Indeed, it has been shown that, without preconditioning, the accuracy of the numerical solution is deteriorated for low Mach numbers, and this up to Mach number values that are hardly reachable for liquid flows. The proposed preconditioning technique appears to be able to eliminate this problem, also for very low Mach numbers (of the order of  $10^{-4}$ - $10^{-5}$ ). However, preconditioning dramatically reduces the time step allowed by the stability of the explicit time advancing; for the lowest considered values of  $M$  the allowable  $\Delta t$  is reduced of several order of magnitudes with respect to non preconditioned simulations. From our results it is clear that 3D simulations of low Mach number barotropic flows are hardly affordable. On the other hand, it has been shown that the proposed implicit time advancing almost completely overcomes this problem. Indeed, for non cavitating cases, the  $\Delta t$  can be increased almost indefinitely; when cavitation phenomena occur, although the gain is more limited because of the stiffness of the problem, the allowable  $\Delta t$  is of the same order as that of explicit non preconditioned simulations and, thus, the deteriorating effect of preconditioning on time stability is eliminated.

Next step will be the implementation of the described numerical approach in a 3D solver based on a mixed finite-element/finite-volume formulation applicable to unstructured grids.

## Acknowledgements

The present study has been funded by the Italian Space Agency (ASI) under the research project FAST2, as sub-contractor of CIRA (CR 10/2002). We wish also to thank H. Guillard for having given us the starting input for the low Mach number analysis and A. Dervieux for many precious discussions.

## References

- [1] R. Abgrall, "An extension of Roe's upwind scheme to algebraic equilibrium real gas models", *Computers and Fluids*, **19**, 171-182 (1991).
- [2] O. Coutier-Delgosha, J.L. Reboud and Y. Delannoy, "Numerical simulation of the unsteady behaviour of cavitating flows", *International Journal for Numerical Methods in Fluids*, **42**/5, 527-548 (2003).
- [3] L. d'Agostino et al., "A Modified Bubbly Isenthalpic Model for Numerical Simulation of Cavitating Flows", *37th AIAA/ASME/SAE/ASEE Joint Propulsion Conference*, Salt Lake City, UT, USA, July 8-11 (2001).
- [4] L. Fezoui and B. Stoufflet, "A class of implicit upwind schemes for Euler simulations with unstructured meshes", *Journal of Computational Physics*, **84**, 174-206 (1989).
- [5] P. Glaister, "An approximate linearised Riemann Solver for the Euler equations for real gases", *Journal of Computational Physics*, **74** 382-408 (1988).

- [6] P. Glaister, "A Riemann Solver for barotropic flow", *Journal of Computational Physics*, **93** 477-480 (1991).
- [7] A. Guardone and L. Vigevano, "Roe linearization for the van der Waals gas", *Journal of Computational Physics*, **175**, 50-78 (2002).
- [8] H. Guillard and C. Viozat, "On the behaviour of upwind schemes in the low Mach number limit", *Computers and Fluids* **28**, 63-86 (1999).
- [9] K.C. Karki and S.V. Patankar, "Pressure based calculation procedure for viscous flows at all speed in arbitrary configurations", *AIAA Journal*, **27/9**, 1167-1174 (1989).
- [10] J.J. McGurick and G.J. Page, "Shock-capturing using a pressure correction method", *AIAA Journal*, **28/10**, 1751-1757 (1989).
- [11] W. H. Press et al., "Numerical Recipes in FORTRAN" , Cambridge University Press (1992).
- [12] P.L. Roe, "Approximate Riemann Solvers, Parameters Vectors, and Difference Schemes", *Journal of Computational Physics* **43**, 357-372 (1981).
- [13] I. Senocak and W. Shyy, "A pressure-based method for turbulent cavitating flow computations", *Journal of Computational Physics*, **176**, 363-383 (2002).
- [14] E. Sinibaldi, *FAST2 Attività di Cavitazione 3D, Technical Report RT1: thermal cavitation model for liquid propellant rocket applications* (2003).
- [15] J.L. Steger and R.F. Warming, "Flux vector splitting for the inviscid gas dynamic equations with applications to finite difference methods", *Journal of Computational Physics*, **40**: 263-293 (1981).
- [16] E. Turkel, "Preconditioned methods for solving the incompressible and low speed compressible equations", *Journal of Computational Physics*, **72**, 277-298 (1987).
- [17] E. Turkel, A. Fiterman and B. van Leer, "Preconditioning and the limit of the compressible to the incompressible flow equations for finite difference schemes", *Frontiers of Computational Fluid Dynamics*, D.A. Caughey and M.M. Hafez Eds.: 215-234, Chichester, Wiley (1994).
- [18] E. Turkel, "Preconditioning techniques in Computational Fluid Dynamics", *Annual Review of Fluid Mechanics*, **31** (1999).
- [19] D.R. Van der Heul, P. Vuik and P. Wesseling, "Efficient computation of flow with cavitation by compressible pressure correction", *ECCOMAS'2000*, Barcelona, Sept. 2000.
- [20] M. Vinokur and J-L Montagné, "Generalized flux-vector splitting and Roe average for an equilibrium real gas", *Journal of Computational Physics*, **89** 276-300 (1990).
- [21] C. Viozat, "Implicit Upwind Schemes for Low Mach Number Compressible Flows", *Rapport INRIA n° 3084* (1997).
- [22] P. Wesseling, D.R. Van der Heul and C. Vuik, "Unified methods for computing compressible and incompressible flows", *ECCOMAS'2000*, Barcelona, Sept. 2000.

## A Proof of Lemma 1

Firstly, by using the classical Roe averages the following algebraic system is satisfied:

$$\begin{pmatrix} 0 & 1 & 0 \\ -\tilde{u}^2 & 2\tilde{u} & 0 \\ -\tilde{u}\tilde{h}_t & \tilde{h}_t & \tilde{u} \end{pmatrix} \begin{pmatrix} \Delta^{lr}(\rho) \\ \Delta^{lr}(\rho u) \\ \Delta^{lr}(\rho h_t) \end{pmatrix} = \begin{pmatrix} \Delta^{lr}(\rho u) \\ \Delta^{lr}(\rho u^2) \\ \Delta^{lr}(\rho h_t u) \end{pmatrix}$$

Therefore, by using this relation, property 3 in Sec. 3.1 may be satisfied as follows:

$$\begin{pmatrix} 0 & 1 & 0 \\ \omega - \tilde{u}^2 & 2\tilde{u} & 0 \\ \tilde{u}(\omega - \tilde{h}_t) & \tilde{h}_t & \tilde{u} \end{pmatrix} \Delta^{lr} W = \Delta^{lr}(F(W))$$

for  $\omega$  verifying:

$$\omega \Delta^{lr} \rho = \Delta^{lr} p \quad (64)$$

If  $\rho_l = \rho_r$  then Eq. (64) is verified for any choice of  $\omega$  while, for  $\rho_l \neq \rho_r$  the only solution is:

$$\omega = \frac{\Delta^{lr} p}{\Delta^{lr} \rho}$$

It is possible to rewrite the above expression as:

$$\omega = \frac{p(\rho_l + \Delta^{lr} \rho) - p(\rho_l)}{(\rho_l + \Delta^{lr} \rho) - \rho_l}$$

thus, by assuming that the barotropic state law is continuously differentiable, the following relation may be derived:

$$\lim_{W_l, W_r \rightarrow W^*} \omega = \lim_{W_l \rightarrow W^*} \lim_{\Delta^{lr} \rho \rightarrow 0} \omega = \lim_{W_l \rightarrow W^*} \frac{dp}{d\rho}(\rho_l) = \frac{dp}{d\rho}(\rho^*) = a^2(\rho^*) \quad (65)$$

We can use Eq.(65) in order to extend (continuous prolongation)  $\omega$  to the case  $\rho_l = \rho_r$ :

$$\omega(W_l, W_r) = \begin{cases} \frac{\Delta^{lr} p}{\Delta^{lr} \rho} & \text{if } \rho_l \neq \rho_r \\ a^2(\rho, p(\rho)) & \text{if } \rho_l = \rho_r = \rho \end{cases}$$

In such a way, also property 2 in Sec. 3.1 is trivially satisfied. By assumption (see Sec. 2),  $P$  is a strictly increasing monotonous function of  $\rho$ , thus,  $\omega$  is always strictly positive. Then, the symbol  $\omega$  can be replaced by  $\tilde{a}^2$ , and in this way, the proposed matrix is exactly the one expressed in (8). Property 1 in Sec. 3.1 is also satisfied: indeed, its eigenvalues are real and equal respectively to  $\tilde{u}$ ,  $\tilde{u} + \tilde{a}$  and  $\tilde{u} - \tilde{a}$  (with  $\tilde{a} = \sqrt{\tilde{a}^2}$ ). This ends the proof.

## B Proof of Lemma 2

Let us consider, at a preliminary stage, a generic function  $G = G(U, V)$ . In order to simplify the notation, let us introduce the following definitions (directly derived from those of Sec. 6.1):

$$\left\{ \begin{array}{l} \Delta_U G = G(U, V_0) - G(U_0, V_0) \\ \Delta_V G = G(U_0, V) - G(U_0, V_0) \\ \bar{\Delta}_U G = G(U_0, V) - G(U, V) \\ \bar{\Delta}_V G = G(U, V_0) - G(U, V) \\ \Delta_{UV} G = G(U, V) - G(U_0, V_0) \end{array} \right.$$

Furthermore, let us prove the following lemma:

**Lemma 3** *Let  $H_1, H_2$  be two matrices and let  $r$  be a vector associated with  $G$  verifying the following equation:*

$$\Delta_U G + \Delta_V G = H_1(U, V_0)(U - U_0) + H_2(U_0, V)(V - V_0) + r(U_0, V_0, U, V) \quad (66)$$

for any value of  $U_0, V_0, U$  and  $V$ . Then, the following relation is satisfied:

$$\Delta_{UV} G = H_1(U_0, V_0)(U - U_0) + H_2(U_0, V_0)(V - V_0) + R(U_0, V_0, U, V) \quad (67)$$

with:

$$\begin{aligned} 2R(U_0, V_0, U, V) = & (\Delta_U H_1 + \Delta_V H_1)(U - U_0) + (\Delta_U H_2 + \Delta_V H_2)(V - V_0) \\ & - \Delta_{UV} r(\cdot, \cdot, U_0, V) - \Delta_{UV} r(\cdot, \cdot, U, V_0) \end{aligned}$$

Proof:

By choosing  $V = V_0$  in (66) one obtains:

$$\Delta_U G = H_1(U, V_0)(U - U_0) + r(U_0, V_0, U, V_0) \quad (68)$$

while for  $U = U_0$  in (66) one obtains:

$$\Delta_V G = H_2(U_0, V)(V - V_0) + r(U_0, V_0, U_0, V) \quad (69)$$

Furthermore, by inverting the role of  $(U_0, V_0)$  and  $(U, V)$  it follows that:

$$\bar{\Delta}_U G = H_1(U_0, V)(U_0 - U) + r(U, V, U_0, V) \quad (70)$$

$$\bar{\Delta}_V G = H_2(U, V_0)(V_0 - V) + r(U, V, U, V_0) \quad (71)$$

From the relevant definitions,  $\Delta_{UV}$  can be also rewritten as:

$$\Delta_{UV}G = \frac{1}{2}(\Delta_U G + \Delta_V G - \bar{\Delta}_U G - \bar{\Delta}_V G) \quad (72)$$

Then, by substituting Eqs. (68), (69), (70) and (71) into Eq. (72) (67) is easily obtained (67). The proof is therefore completed.

We can now prove Lemma 2. Indeed, from (48) we know that the Roe flux function can be expressed as follows:

$$\Phi(U, V) = \begin{cases} \frac{F(U) + F(V)}{2} - \frac{1}{2} |\tilde{A}(U, V)| (V - U) \\ F(U) + \tilde{A}^-(U, V) (V - U) \\ F(V) - \tilde{A}^+(U, V) (V - U) \end{cases}$$

Thus, in particular:

$$\begin{cases} \Phi(U_0, V_0) = F(U_0) + \tilde{A}^-(U_0, V_0) (V_0 - U_0) \\ \Phi(U_0, V) = F(U_0) + \tilde{A}^-(U_0, V) (V - U_0) \end{cases} \quad (73)$$

$$\begin{cases} \Phi(U_0, V_0) = F(V_0) - \tilde{A}^+(U_0, V_0) (V_0 - U_0) \\ \Phi(U, V_0) = F(V_0) - \tilde{A}^+(U, V_0) (V_0 - U) \end{cases} \quad (74)$$

From Eqs. (73) and (74) one obtains:

$$\begin{cases} \Delta_U \Phi = -\tilde{A}^+(U, V_0) (V_0 - U) + \tilde{A}^+(U_0, V_0) (V_0 - U_0) \\ \Delta_V \Phi = \tilde{A}^-(U_0, V) (V - U_0) - \tilde{A}^-(U_0, V_0) (V_0 - U_0) \end{cases}$$

and:

$$\Delta_U \Phi + \Delta_V \Phi = \tilde{A}^+(U, V_0) (U - U_0) + \tilde{A}^-(U_0, V) (V - V_0) + r^{Roe}(U_0, V_0, U, V) \quad (75)$$

where:

$$r^{Roe}(U_0, V_0, U, V) = (\Delta_V \tilde{A}^- - \Delta_U \tilde{A}^+) (V_0 - U_0)$$

Note that:

$$\begin{aligned} \Delta_{UV} r^{Roe}(\cdot, \cdot, U_0, V) &= r^{Roe}(U, V, U_0, V) - r^{Roe}(U_0, V_0, U_0, V) \\ &= -\bar{\Delta}_U \tilde{A}^+ (V - U) - \Delta_V \tilde{A}^- (V_0 - U_0) \end{aligned}$$

$$\begin{aligned}\Delta_{UV} r^{Roe}(\cdot, \cdot, U, V_0) &= r^{Roe}(U, V, U, V_0) - r^{Roe}(U_0, V_0, U, V_0) \\ &= \bar{\Delta}_V \tilde{A}^-(V - U) + \Delta_U \tilde{A}^+(V_0 - U_0)\end{aligned}$$

Finally, by applying Lemma 3 with  $H_1 = \tilde{A}^+$ ,  $H_2 = \tilde{A}^-$  and  $r = r^{Roe}$ , it follows that:

$$\Delta_{UV} \Phi = \tilde{A}^+(U_0, V_0)(U - U_0) + \tilde{A}^-(U_0, V_0)(V - V_0) + R \quad (76)$$

where  $R = R(U_0, V_0, U, V)$  is given by:

$$\begin{aligned}2R &= (\Delta_U \tilde{A}^+ + \Delta_V \tilde{A}^+) (U - U_0) \\ &\quad + (\Delta_U \tilde{A}^- + \Delta_V \tilde{A}^-) (V - V_0) \\ &\quad + (\Delta_V \tilde{A}^- - \Delta_U \tilde{A}^+) (V_0 - U_0) \\ &\quad + (\bar{\Delta}_U \tilde{A}^+ - \bar{\Delta}_V \tilde{A}^-) (V - U)\end{aligned}$$

By means of an immediate change of notation, it is possible to recognize that (76) is formally identical to (54). This completes the proof.

## C Numerical implementation of the mixture barotropic law

The mixture barotropic law can be computed and stored at the beginning of each simulation and the required output can be interpolated for the given value of the independent variable as required by the simulation algorithm. As a result, a reduction in the computational time is attained at the cost of a relatively small amount of data storage. However, in a density-based CFD solver it is possible to render the interpolation procedure:  $\rho \mapsto (p, a)$  more efficient by pre-processing the mixture barotropic law as follows:

- at a first stage Eq. (62) is integrated with respect to  $p$  (in order to mitigate the numerical stiffness) by exploiting a fourth-order Runge-Kutta method with adaptive stepsize control [11]. Three sequences are produced as output:  $\rho_i$ ,  $a_i$  and  $p_i$  ( $i = 1, \dots, n$ ), describing the mixture sound speed curve  $a_i(\rho_i)$  and the corresponding barotropic law  $p_i(\rho_i)$ ;
- at a second stage a new density sequence  $\rho'_i$  ( $i = 1, \dots, n$ ) is derived from  $\rho_i$  in order to simplify the interpolation procedure, as described below. A new pressure sequence  $p'_i$  as well as a new sound speed sequence  $a'_i$  are then determined by linear interpolation of  $p_i(\rho_i)$  and  $a_i(\rho_i)$ , respectively, with respect to the sampling sequence  $\rho'_i$ . The resulting curves,  $p'_i(\rho'_i)$  and  $a'_i(\rho'_i)$ , closely approximate  $p_i(\rho_i)$  and  $a_i(\rho_i)$ , respectively, and constitute the interpolation database to be used by the density-based CFD solver.

From the above discussion it is clear that the sampling sequence  $\rho'_i$  should be a good approximation of  $\rho_i$  (so that  $p'_i(\rho'_i)$  preserves the main features of the mixture barotropic law) while simplifying the interpolation procedure. In order to introduce a suitable definition of  $\rho'_i$ , let consider the density spacing  $(\rho_{i+1} - \rho_i)$ . It is negative because the mixture barotropic law, which is monotonic, has been obtained by integrating Eq. (62) from  $\rho_1 = \rho_{lsat}$  to  $\rho_n \ll \rho_{lsat}$ . In addition, it shows a typical behavior (see Fig. 9):

- its absolute value decreases as  $i \rightarrow 1$  ( $\alpha \rightarrow 0$ ) or  $i \rightarrow n$  ( $\alpha \rightarrow 1$ );
- it is roughly symmetrical with respect to a certain value  $\rho^* \simeq \rho_1/2$ .

It may be worth noting that both these features are due to the adaptive nature of the proposed integration routine, together with the fact that the mixture barotropic law exhibits abrupt changes in its gradient near the pure liquid and pure vapor extreme and it is roughly symmetrical with respect to the point ( $\alpha \simeq 0.5, p(\alpha \simeq 0.5)$ ).

In consideration of the above features, it seems reasonable to define  $\rho'_i$  by means of two geometric subsequences,  $\rho_i^{(1)}$  and  $\rho_i^{(2)}$ , starting from  $\rho_1$  and  $\rho_n$ , respectively, and joining together at a common element in between. Indeed, these subsequences can approximate the spacing distribution of  $\rho_i$  and, at the same time, analitically provide the interpolation interval  $(\rho'_{i+1}, \rho'_i)$  that contains any given input density  $\rho_n \leq \rho \leq \rho_1$ , as described below.

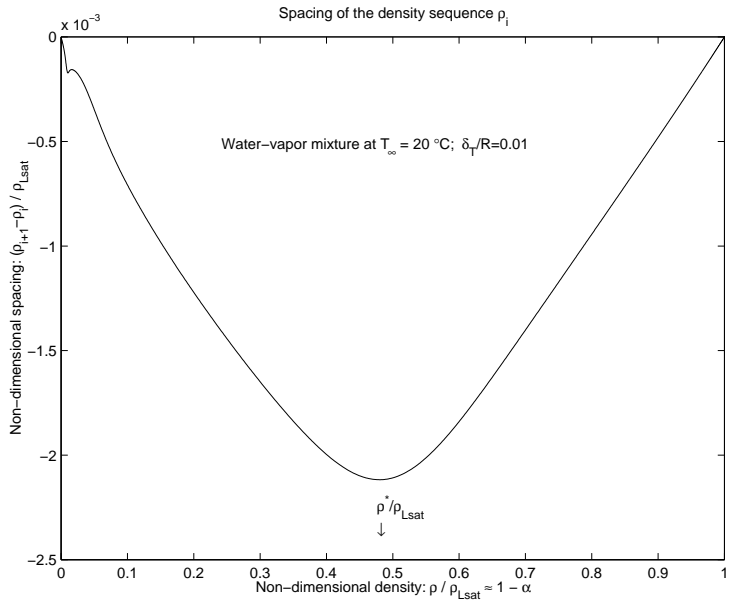


Figure 9: Typical behavior of the density spacing  $(\rho_{i+1} - \rho_i)$  as a function of the liquid fraction  $(1 - \alpha)$  for a water-vapor mixture at  $T_\infty = 20^\circ\text{C}$ , with  $\delta_T/R = 0.01$

Let  $q_1 > 1$  and  $q_2 > 1$  be the “ratios” and let  $\delta_1 > 0$  and  $\delta_2 > 0$  be the “initial spacings” associated with  $\rho_i^{(1)}$  and  $\rho_i^{(2)}$ , respectively. A possible definition of  $\rho'_i$  is therefore:

$$\rho'_i = \begin{cases} \rho_i^{(1)} = \rho_1 - \frac{q_1^{i-1} - 1}{q_1 - 1} \delta_1 & \text{if } i = 1, \dots, p \\ \rho_i^{(2)} = \rho_n + \frac{q_2^{n-i} - 1}{q_2 - 1} \delta_2 & \text{if } i = p, \dots, n \end{cases}$$

It is possible to relate  $q_1$  to  $\delta_1$  and  $q_2$  to  $\delta_2$  by imposing a compatibility constraint of the form:

$$\rho_p^{(1)} = \rho_p = \rho_p^{(2)}$$

where  $\rho_p$  is the  $p$ -th element of  $\rho_i$ . The specific value of  $\rho_p$  can be determined from the relation:

$$\rho_{p+1} < \rho^* < \rho_p$$

where  $\rho^*$  is considered as an input parameter of the pre-processing strategy under discussion. However, it is worth observing that the resulting curve  $p'_i(\rho'_i)$  is not very sensitive to the exact value of  $\rho^*$  because the mixture barotropic law flattens far from the pure liquid and

pure vapor extreme.

Once the control parameters  $q_1$  (or  $\delta_1$ ) and  $q_2$  (or  $\delta_2$ ) have been given a value,  $\rho'_i$  is completely defined and the sampling process can be performed. The resulting curve  $p'_i = p(\rho'_i)$  is generally very close to  $p_i = p(\rho_i)$ , as shown in Fig. 10, and the same result can be achieved also for the sound speed curves.

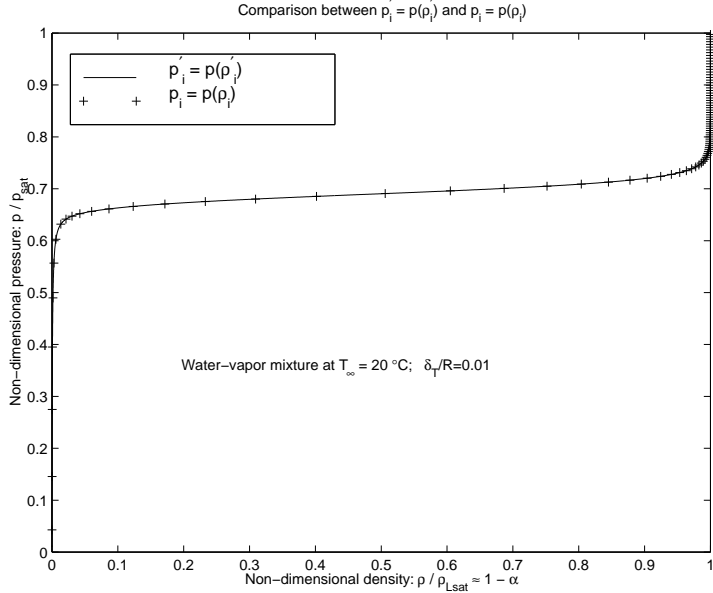


Figure 10: Comparison between  $p'_i = p(\rho'_i)$  and  $p_i = p(\rho_i)$  as a function of the liquid fraction  $(1 - \alpha)$  for a water-vapor mixture at  $T_\infty = 20^\circ\text{C}$ , with  $\delta_T/R = 0.01$

Finally, in correspondence of any given input density  $\rho_n \leq \rho \leq \rho_1$  ( $\rho \neq \rho_p$ ), it is possible to determine an index  $j = j(\rho)$ :

$$j = \begin{cases} \text{int} \left( 1 + \frac{1}{\ln q_1} \ln \left( 1 + \frac{\rho_1 - \rho}{\delta_1} (q_1 - 1) \right) \right) & \text{if } \rho_p < \rho \leq \rho_1 \\ \text{int} \left( (n - 1) - \frac{1}{\ln q_2} \ln \left( 1 + \frac{\rho - \rho_n}{\delta_2} (q_2 - 1) \right) \right) & \text{if } \rho_n \leq \rho < \rho_p \end{cases}$$

which immediately identifies the interval  $(\rho'_j, \rho'_{j+1})$  to be used for the interpolation procedure:  $\rho \mapsto (p, a)$ . More precisely (the case  $\rho = \rho_p$  is trivial):

$$\begin{cases} \rho'_{j+1} < \rho \leq \rho'_j & \text{if } \rho_p < \rho \leq \rho_1 \\ \rho'_{j+1} \leq \rho < \rho'_j & \text{if } \rho_n \leq \rho < \rho_p \end{cases}$$

In conclusion, the pre-processing strategy described in the present section allows an efficient interpolation process to be defined, thus rendering the chosen cavitation model particularly suitable for implementation in a density-based CFD solver.



---

Unité de recherche INRIA Sophia Antipolis  
2004, route des Lucioles - B.P. 93 - 06902 Sophia Antipolis Cedex (France)

Unité de recherche INRIA Lorraine : Technopôle de Nancy-Brabois - Campus scientifique  
615, rue du Jardin Botanique - B.P. 101 - 54602 Villers lès Nancy Cedex (France)

Unité de recherche INRIA Rennes : IRISA, Campus universitaire de Beaulieu - 35042 Rennes Cedex (France)

Unité de recherche INRIA Rhône-Alpes : 655, avenue de l'Europe - 38330 Montbonnot St Martin (France)

Unité de recherche INRIA Rocquencourt : Domaine de Voluceau - Rocquencourt - B.P. 105 - 78153 Le Chesnay Cedex (France)

---

Éditeur

INRIA - Domaine de Voluceau - Rocquencourt, B.P. 105 - 78153 Le Chesnay Cedex (France)

<http://www.inria.fr>

ISSN 0249-6399